

Status of Parton Density Function measurements.

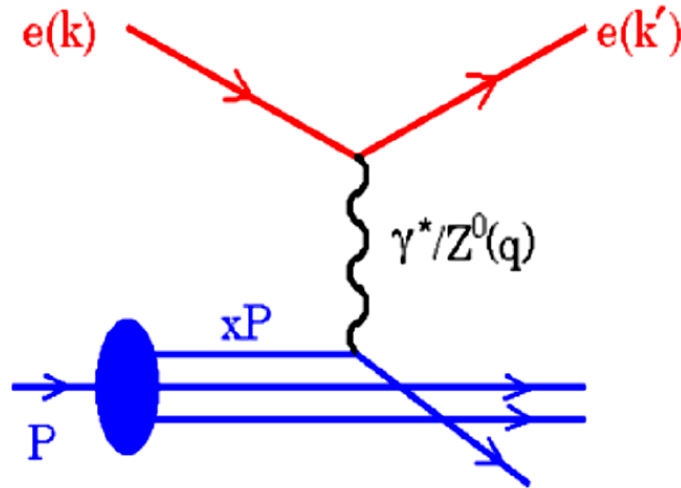
S. Glazov

DESY

ICHEP 2012, Melbourne.

Proton structure probe

Neutral current Deep Inelastic Scattering (DIS) cross section:



$$\frac{d^2\sigma^\pm}{dx dQ^2} = \frac{2\pi\alpha^2 Y_\pm}{Q^4 x} \sigma_r^\pm =$$

$$= \frac{2\pi\alpha^2 Y_\pm}{Q^4 x} \left[F_2(x, Q^2) - \frac{y^2}{Y_\pm} F_L(x, Q^2) \mp \frac{Y_\mp}{Y_\pm} xF_3 \right]$$

where factors $Y_\pm = 1 \pm (1 - y)^2$ and y^2 define polarisation of the exchanged boson and $y = Q^2/(S x)$.

Kinematics is determined by Q^2 and Bjorken x .

At leading order:

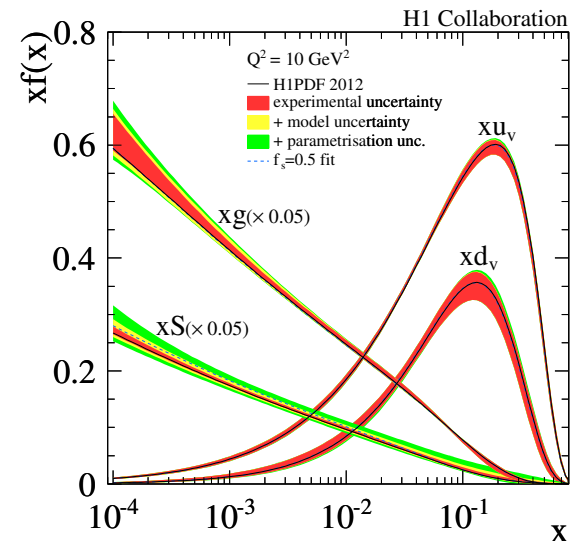
$$F_2 = x \sum e_q^2 (q(x) + \bar{q}(x))$$

$$xF_3 = x \sum 2e_q a_q (q(x) - \bar{q}(x))$$

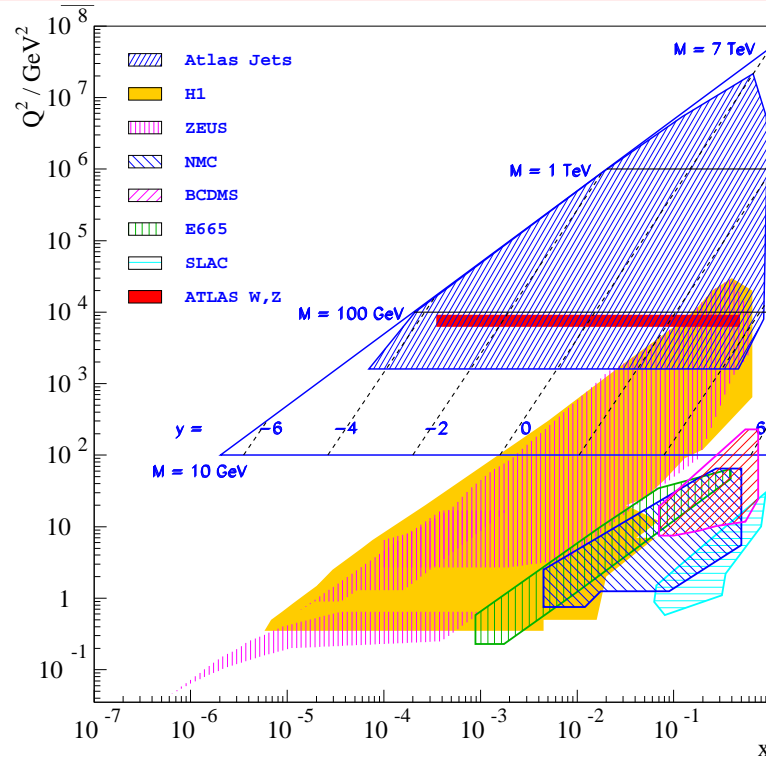
$$\sigma_{CC}^+ \sim x(\bar{u} + \bar{c}) + x(1 - y)^2 (d + s)$$

$$\sigma_{CC}^- \sim x(u + c) + x(1 - y)^2 (\bar{d} + \bar{s})$$

$xg(x)$ — from F_2 scaling violation, jets and F_L



Cross sections at the LHC



The cross sections are given by a convolution of the parton densities and coefficient functions, $\sim x_1 f_1(x_1, \mu) x_2 f_2(x_2, \mu) \hat{\sigma}(x_1, x_2, \mu)$. Leading order relation between rapidity y and x_1, x_2 : $x_{1,2} = \frac{M_{\ell\ell}}{\sqrt{S}} e^{\pm y_{\ell\ell}}$.

Kinematic range of the LHC is covered by the HERA measurements. LHC measurements check validity of pQCD, provide information for PDF decomposition.

→ PDFs have on average > 1.3 citation per LHC paper (estimated based on study of G. Salam, La Thuile 2012)

PDF Sets

Several groups determine PDFs in fits to various data samples:

	MSTW08	CTEQ6.6/CT10	NNPDF2.1/2.3	HERAPDF1.0/1.5	ABKM09/ABM11	GJR08/JR09
Evolution	LO	LO	LO	—	—	—
Order	NLO	NLO	NLO	NLO	NLO	NLO
	NNLO	NNLO	NNLO	NNLO	NNLO	NNLO
HF Scheme	RT-GMVF	ACOT-GMVF	FONLL-GMVF	RT-GMVF (*)	BMSN-FFNS	FFNS
α_S NLO	0.120	0.118(f)	0.1191(b)	0.1176(f)	0.118	0.1135
α_S NNLO	0.1171	0.118(f)	0.1174(b)	0.1176(f)	0.1135	0.1124
HERA DIS	not up-to-date	+	+	+/prelim.	partial	+
Fixed target DIS	+	+	+	-	+	+
DY	+	+	+	-	+	+
Tevatron W,Z	some	some	some	-	some	some
Tevatron jets	some	+	+	-	some	some
LHC	-	-	W, Z+jets (NNPDF2.3)	-	-	-

The analyses differ in many areas:

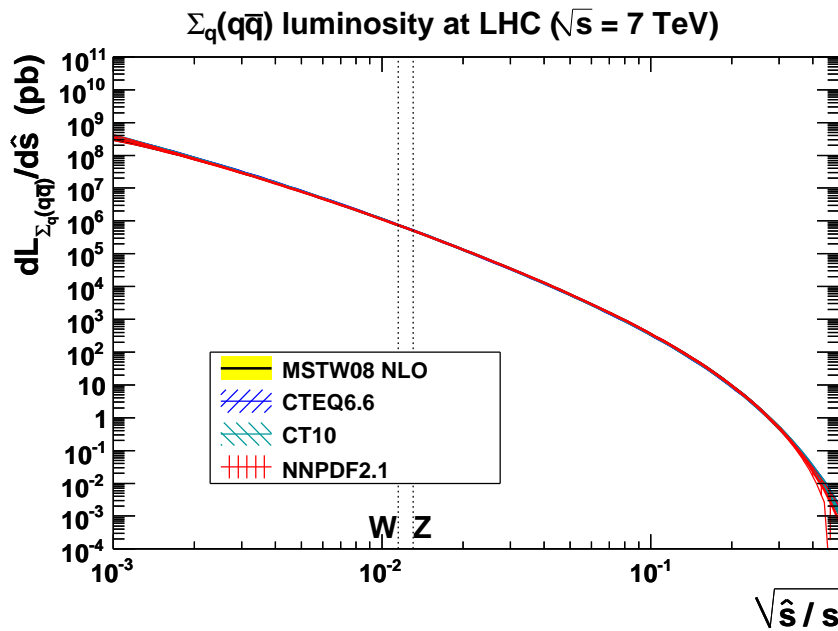
- Higher orders counting (e.g. F_L), heavy flavour corrections, α_S treatment, EW corrections, extra theory assumptions.
- Inclusion of datasets, accounting for data-data-theory tensions.
- PDF parameterisation.

PDF4LHC meetings is a forum to discuss/understand these differences.

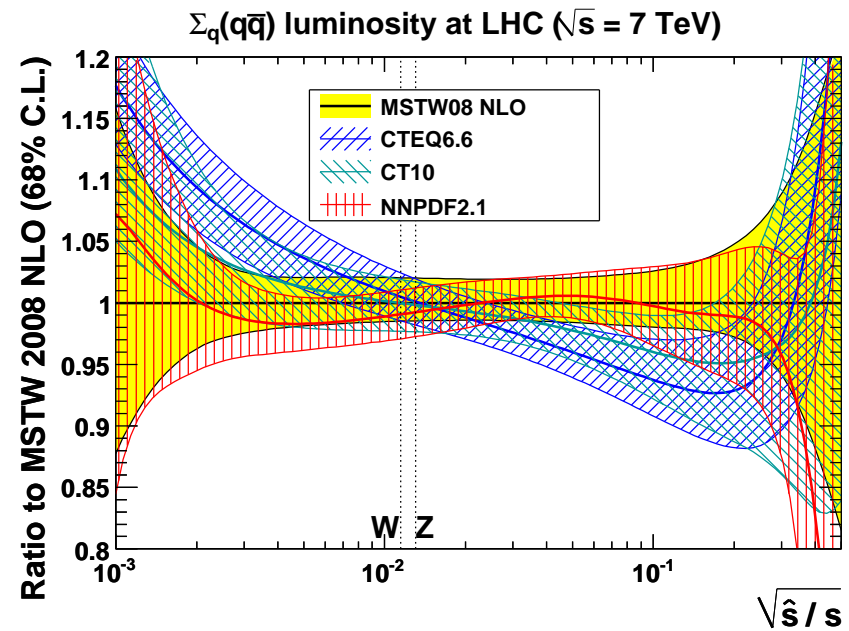
HERAFitter, open source PDF fit project, to study them in details.

arXiv:1101.0536, arXiv:1101.0538

Cross-section predictions for the LHC



G. Watt (March 2011)



G. Watt (March 2011)

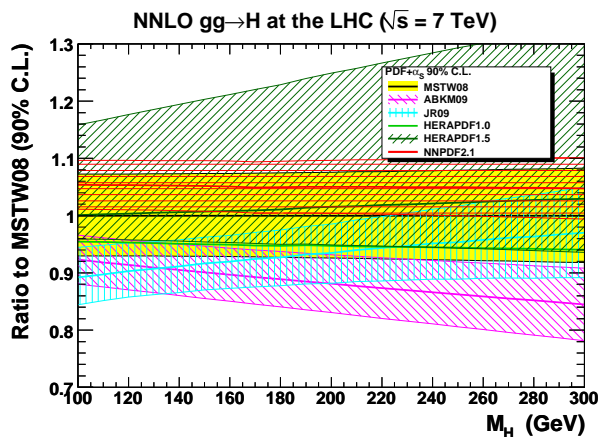
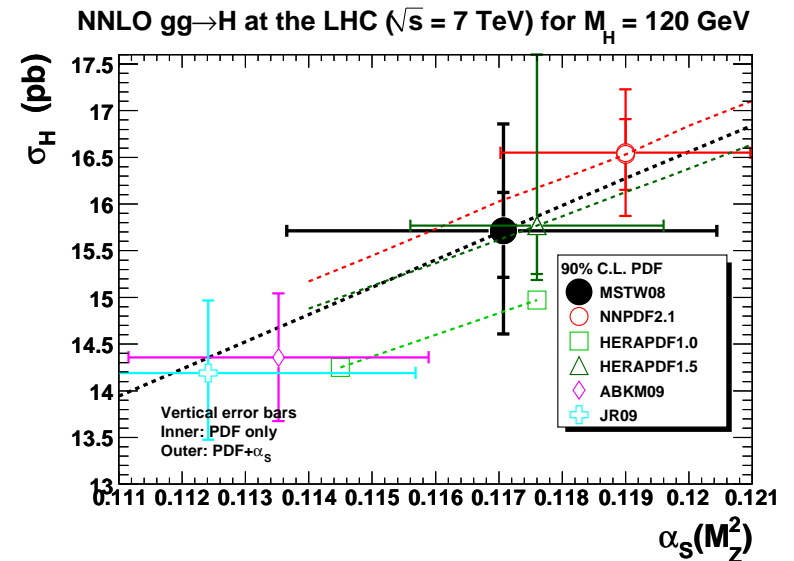
(<http://mstwpdf.hepforge.org/pdf4lhc/partonlumi7TeVnlo.html>), by G. Watt.

- $q\bar{q}$ luminosity, mostly relevant for DY (W, Z production) total cross section, S -channel processes.
- Overall good agreement between predictions over many orders of magnitude. However differences up to 10% level for the ratios.

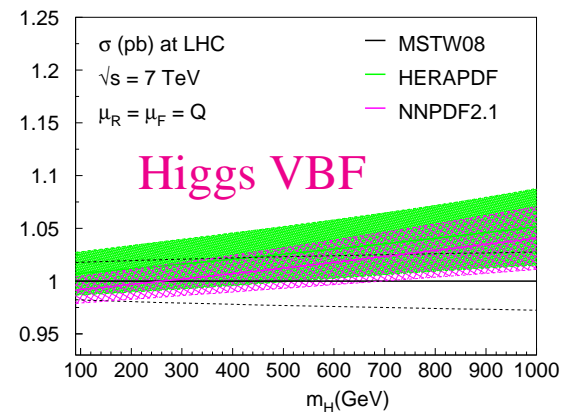
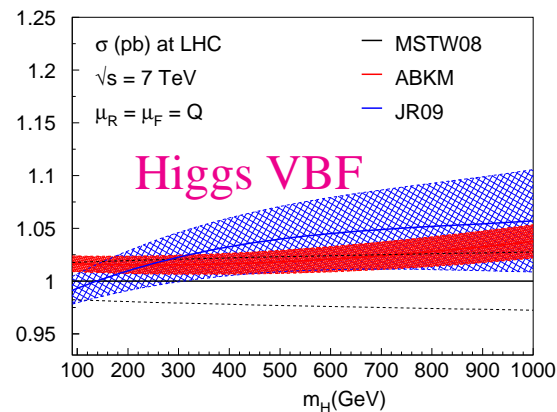
For $M_h = 126$ GeV, $\sqrt{\hat{s}}/s \approx 0.02$ which corresponds to Bjorken- x of the central Higgs production.

Cross-section predictions at the LHC: Higgs

- Uncertainties for the dominant $gg \rightarrow H$ process are mostly from gluon density and α_S . VBF process given at LO by $qq \rightarrow Hqq$ has smaller uncertainties.
- Overall $\sim 10\%$ agreement for the same α_S . Somewhat larger uncertainty for HERAPDF since no jet data are included.



G. Watt (September 2011)



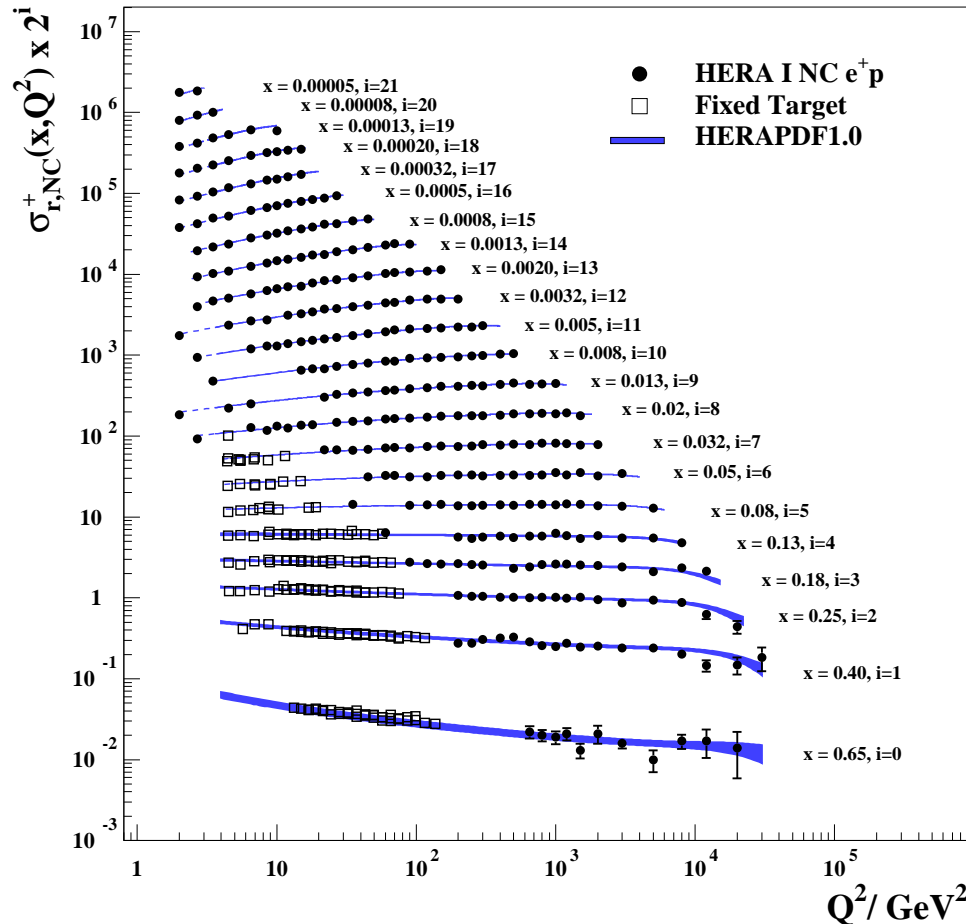
G. Watt, <http://mstwpdf.hepforge.org/pdf4lhc/ringberg>

P. Bolzoni, *et. al.* Phys. Rev. D 85, 035002 (2012), Anastasiou, *et. al.* arXiv:1202.3638.

G. Watt (September 2011)

HERAPDF1.0 fit

H1 and ZEUS



JHEP 1001 (2010) 109.

Good consistency between H1 and ZEUS. Stringent test of DGLAP evolution.

Combination of the published H1/ZEUS data collected at HERA-I for CC,NC, $e^\pm p$ mode. 14 publications, 1402 input and 741 output σ_r measurements, 110 correlated experimental error sources. For NC $e^+ p$, $6 \cdot 10^{-7} < x < 0.65$ and $0.045 < Q^2 < 30000 \text{ GeV}^2$.

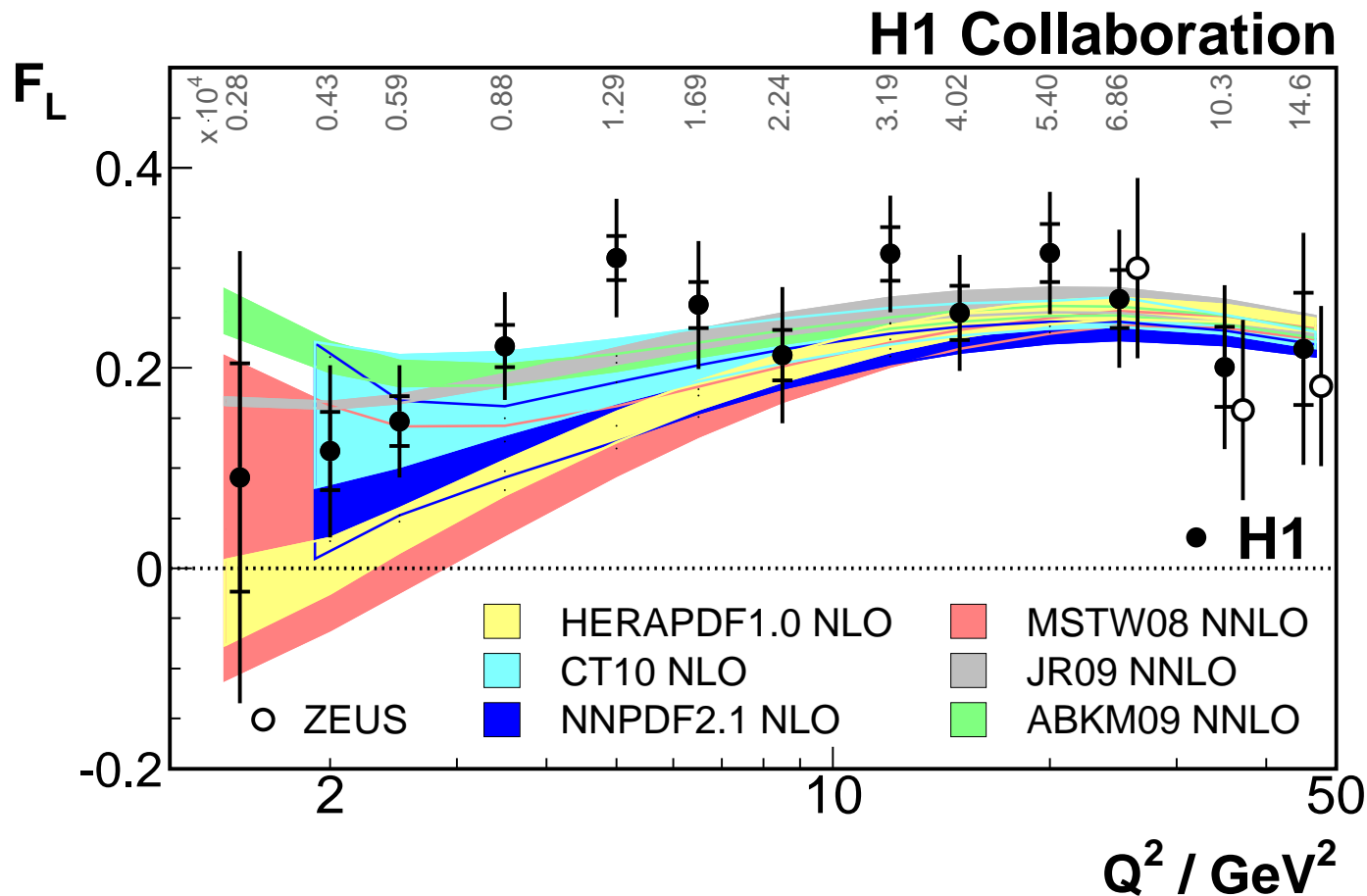
Combination:

$$\chi^2/dof = 637/656$$

QCD Fit (to the combined HERA data with $Q^2 \geq 3.5 \text{ GeV}^2$):

$$\chi^2/dof = 574/582$$

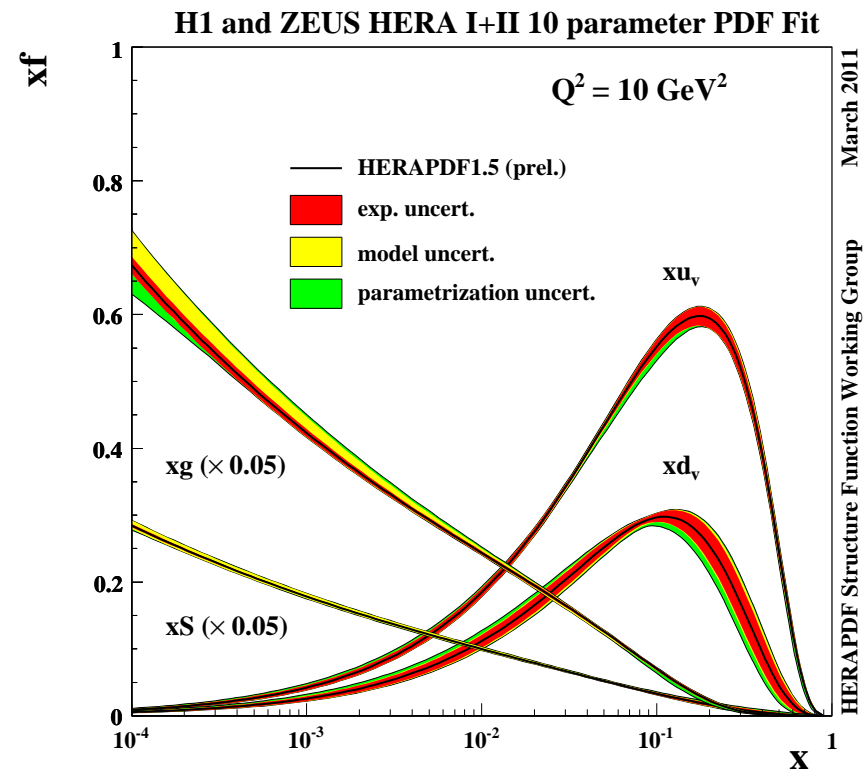
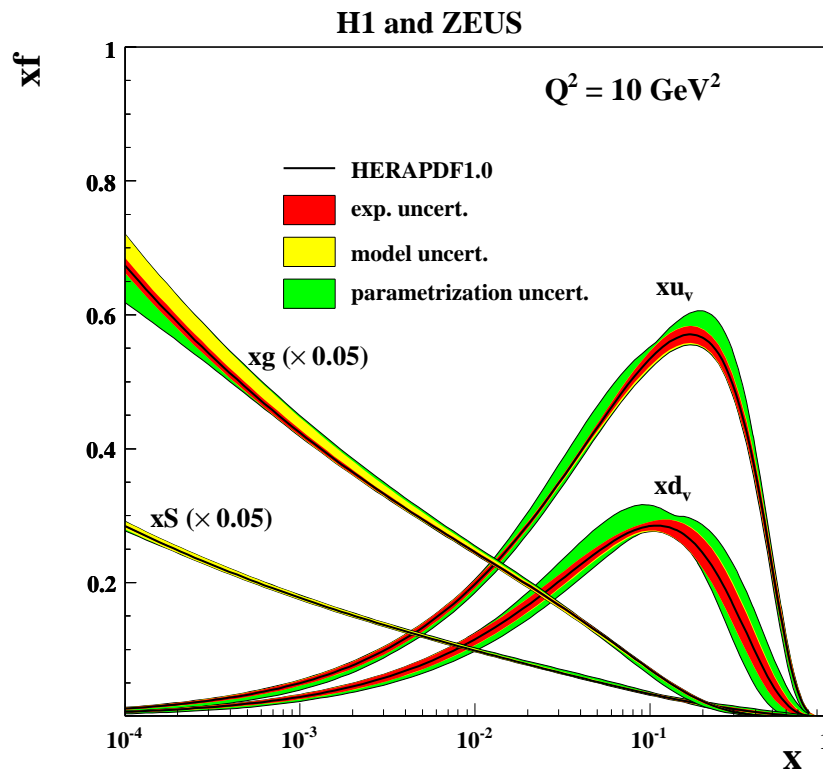
Measurement of the Structure Function F_L



Measurement of the structure function F_L extended to $Q^2 \geq 1.5 \text{ GeV}^2$ and compared to predictions from PDF groups. Good agreement, within the uncertainties. **Critical test** for gluon density.

H1 Collaboration, Eur.Phys.J C71 (2011) 1579

HERAPDF1.0 and HERAPDF1.5 fits

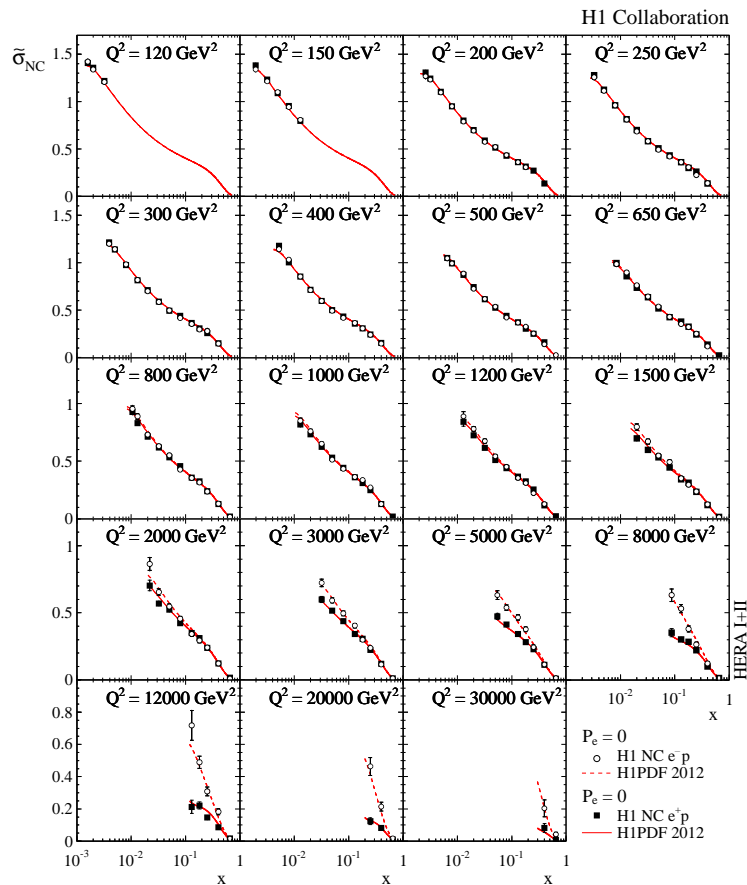


HERAPDF Structure Function Working Group March 2011

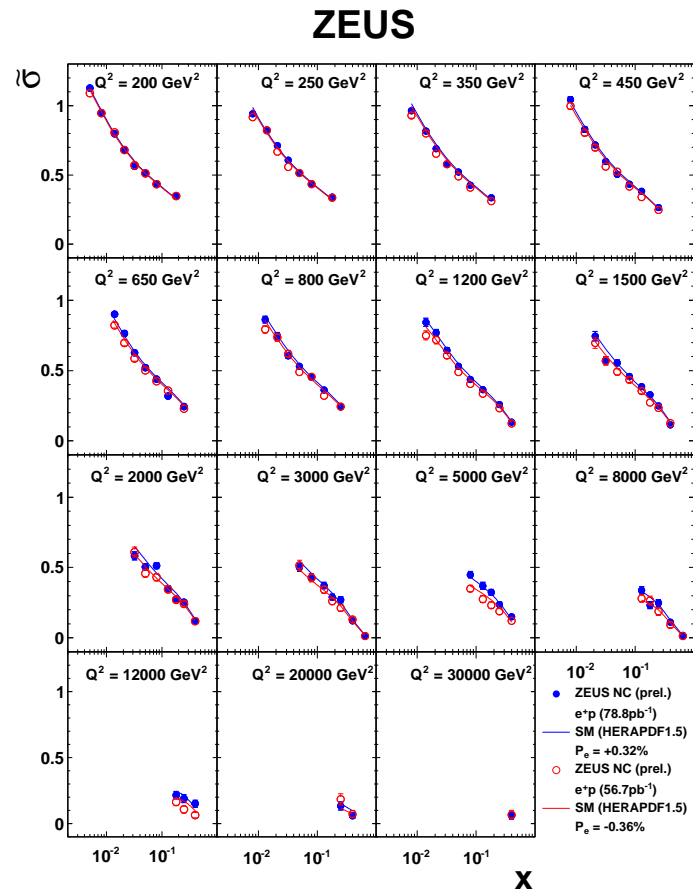
H1prelim-10-142, ZEUS-prel-10-018

- Preliminary combination of H1 and ZEUS complete data samples.
- **Experimental**, **model** and **parameterisation** uncertainties are estimated.
- HERAPDF1.5 fit provides determination of the valence quark densities at high x with reduced uncertainties compared to HERAPDF1.0.

Towards HERAPDF2.0: ZEUS and H12012



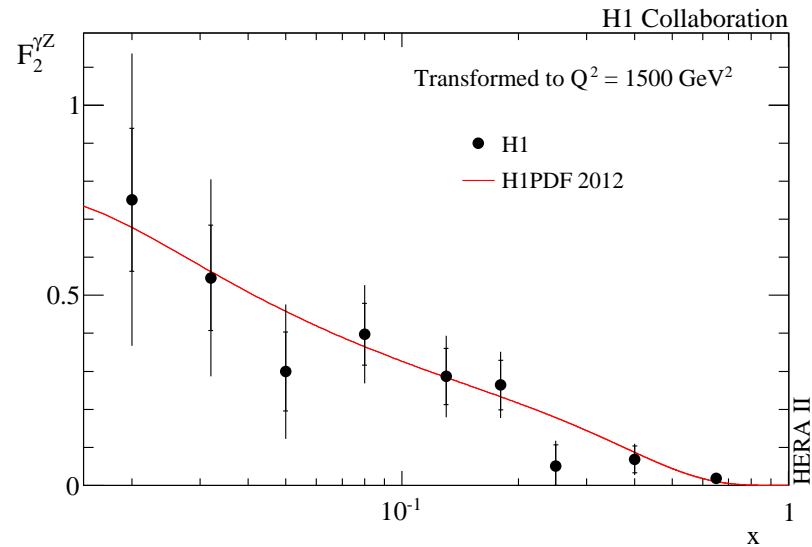
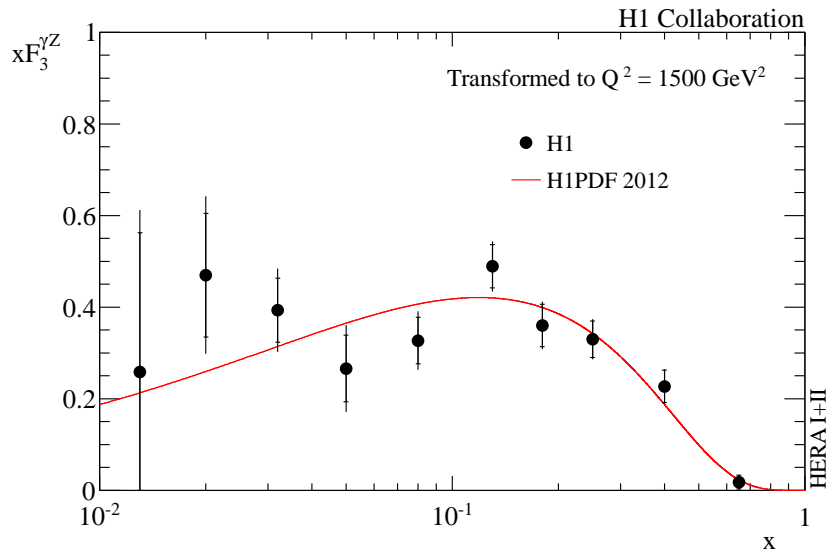
H1 Collaboration, arXiv:1206.7007



ZEUS-prel-11-003

H1 measurement of CC and NC $e^\pm p$ cross sections based on complete HERA sample. ZEUS preliminary result for $e^+ p$ NC cross section, last unpublished result for inclusive measurements at HERA.

H1 measurement of $x F_3^{\gamma Z}$ and $F_2^{\gamma Z}$



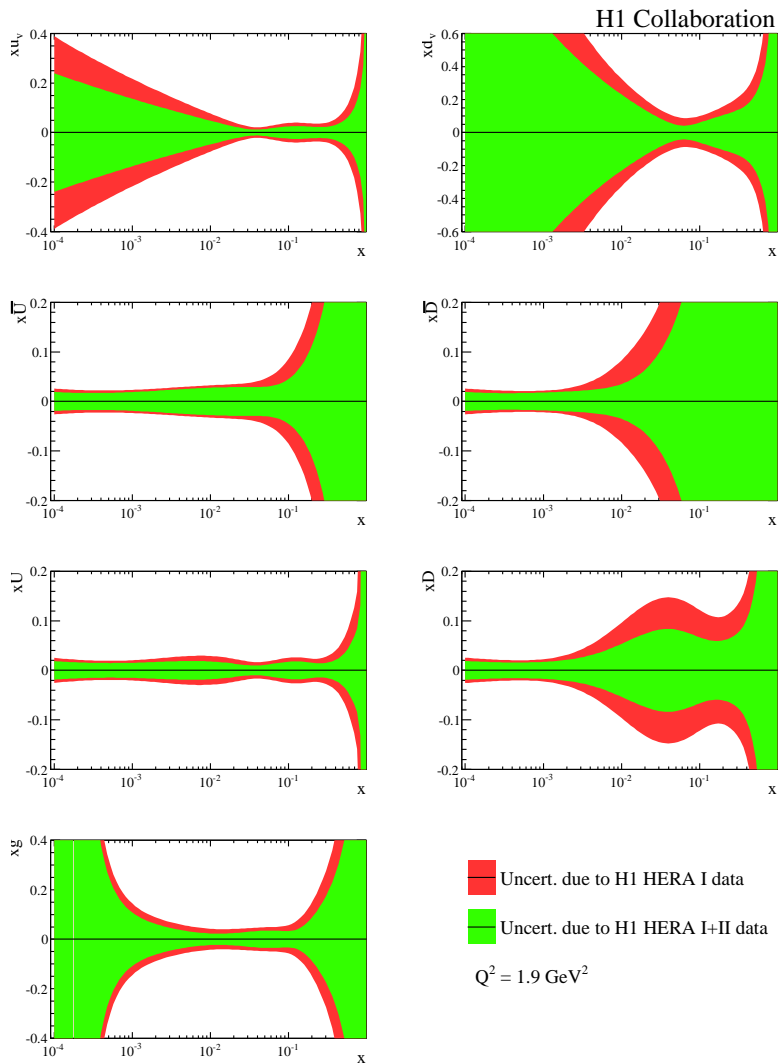
$$\sigma_r^\pm = \tilde{F}_2^\pm \mp \frac{1 - (1 - y)^2}{1 + (1 + y)^2} x \tilde{F}_3 - \frac{y^2}{1 + (1 - y)^2} \tilde{F}_L \quad \tilde{F}_2^\pm \approx F_2 - (v_e \pm P_e a_e) \kappa \frac{Q^2}{Q^2 + M_Z^2} F_2^{\gamma Z}$$

Explore charge asymmetry to extract $x F_3^{\gamma Z}$ and polarisation P_e
 asymmetry to extract $F_2^{\gamma Z}$.

First measurement of the structure function $F_2^{\gamma Z}$.

H1 Collaboration, arXiv:1206.7007

Impact of the HERA-II measurement

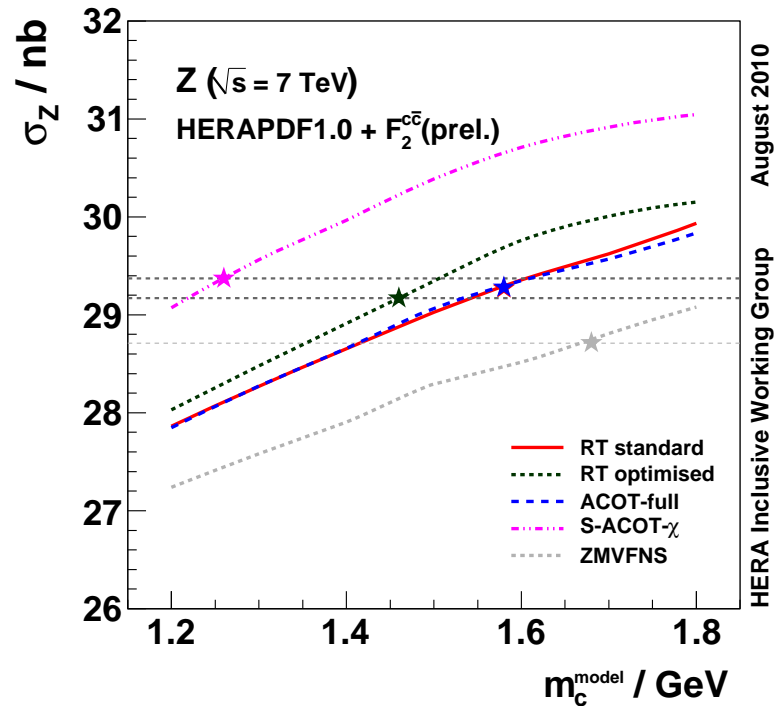
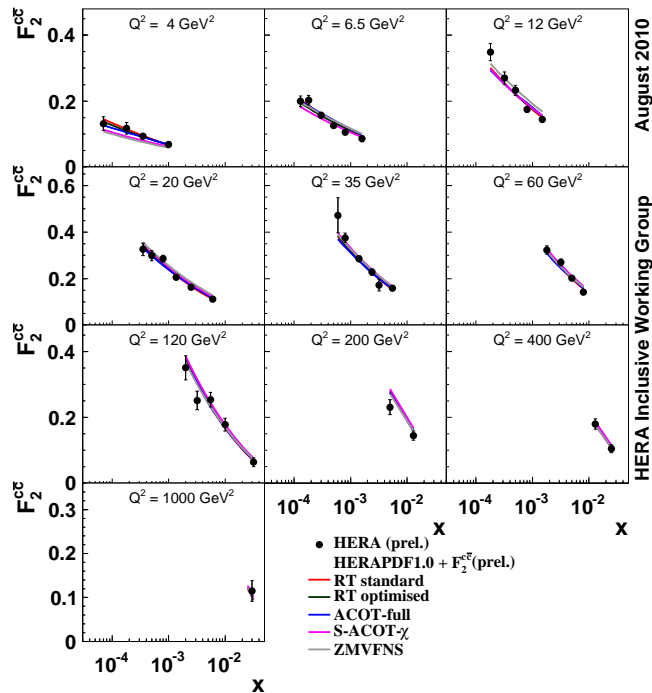


H1 measurement allows to significantly reduce PDF uncertainties at high x , in particular for $D = d + s$ -type quarks.

→ important step towards combination of complete H1 and ZEUS data samples.

H1 Collaboration, arXiv:1206.7007

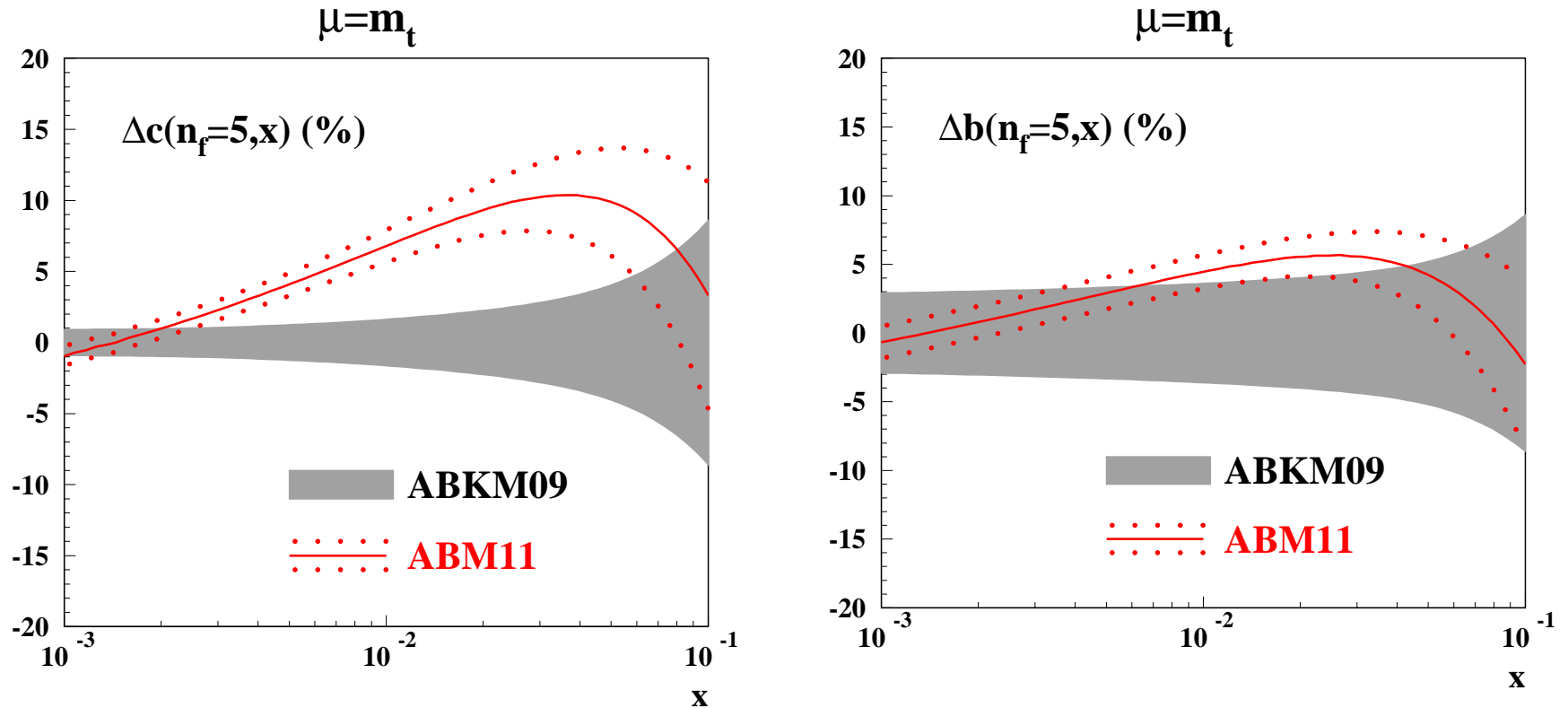
W, Z cross sections and charm-sea density.



Large $\sim 7\%$ spread of the Z total cross section prediction at the LHC for m_c^{model} scan between $1.2 - 1.8 \text{ GeV}$ and also for a fixed m_c^{model} when considering different models. However, the spread is reduced significantly when predictions are evaluated at the $m_c^{\text{model}}(\text{opt})$ values, determined from the fit to HERA F_2^{cc} data.

H1prelim-10-143, ZEUS-prel-10-019

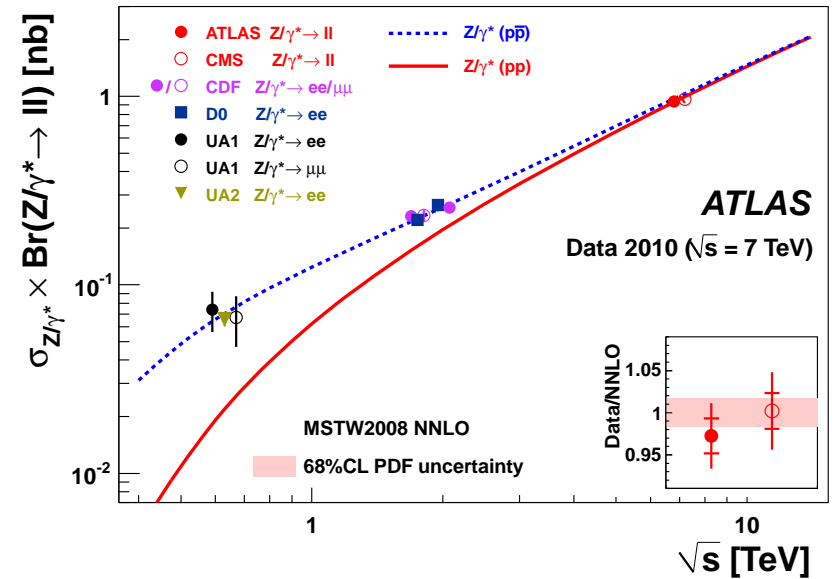
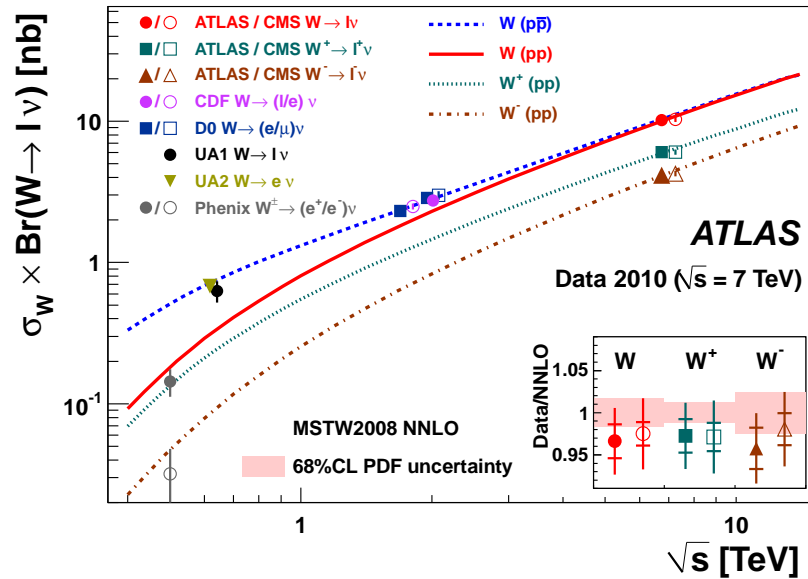
Charm and Bottom densities theory improvements



Theoretical uncertainty in charm and bottom quark densities can be reduced by using $\overline{\text{MS}}$ -scheme for the masses. The scheme is implemented in the recently released ABM11 set. The improvement in b -quark density is important for single top production at the LHC.

S. Alekhin, J. Blümlein, S. Moch, arXiv:1202.2281

W, Z Total cross section results

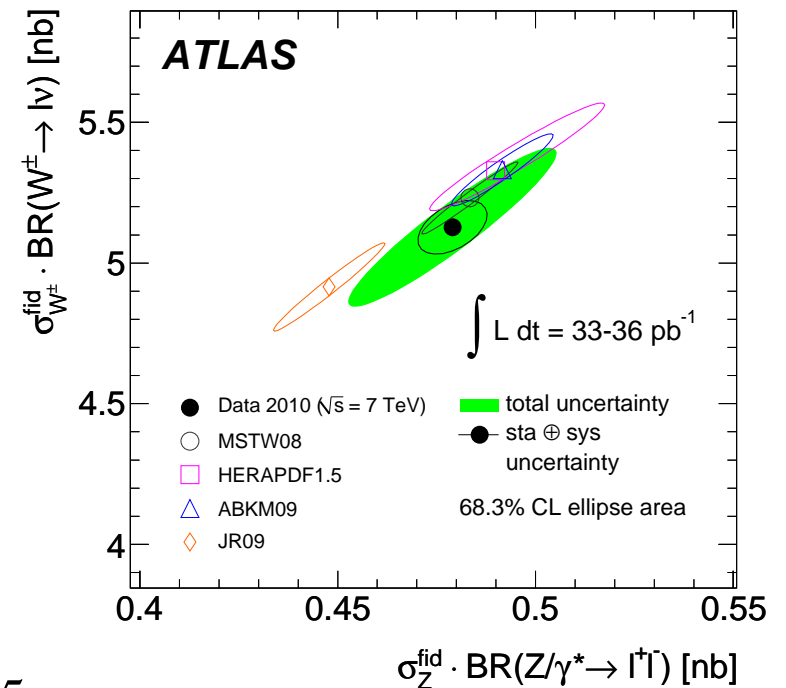


Total cross section measurements for W, Z production at the LHC agree between ATLAS and CMS and also with theoretical predictions.

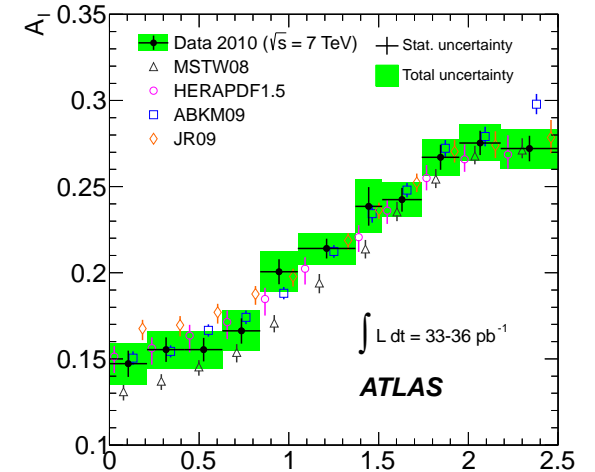
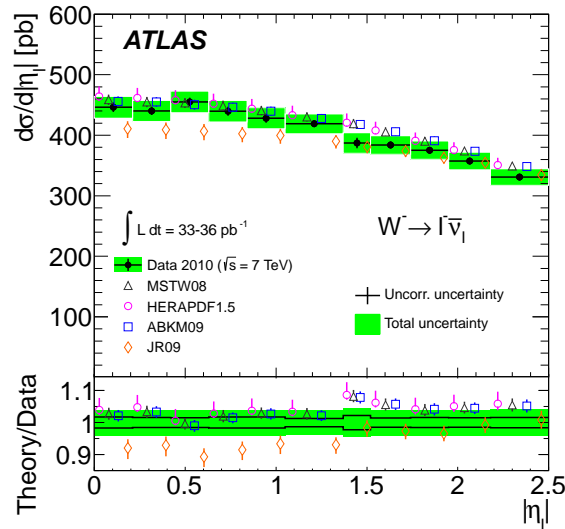
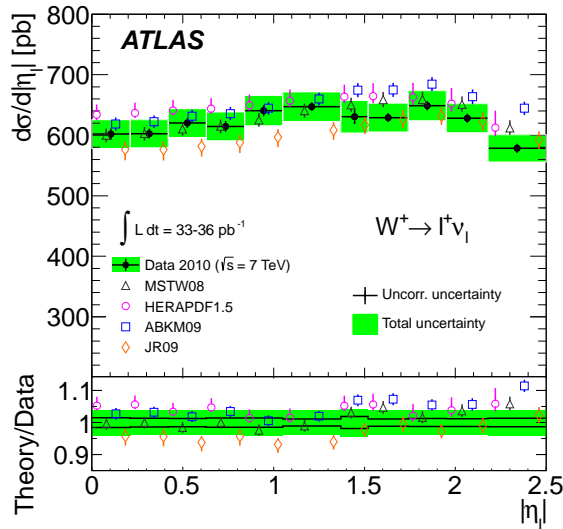
Largest uncertainty is due to luminosity measurement in 2010, 3.4% which improves to 1.8% in 2011.

ATLAS, Phys. Rev. D85 (2012) 072004.

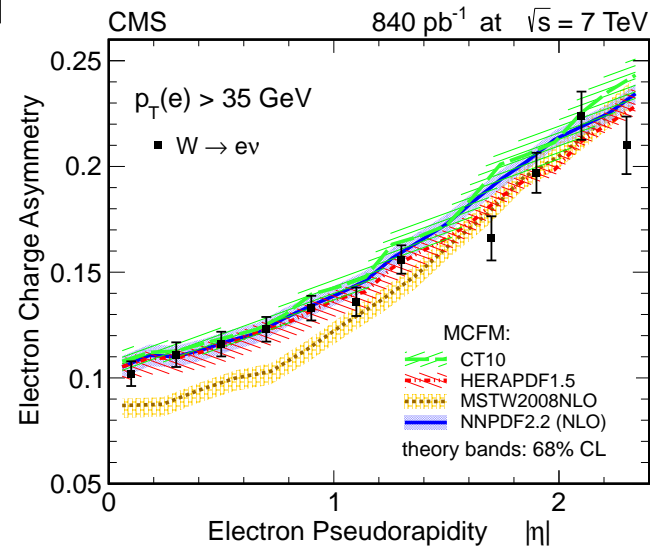
CMS, JHEP 10 (2011) 132.



Differential Cross Sections: W

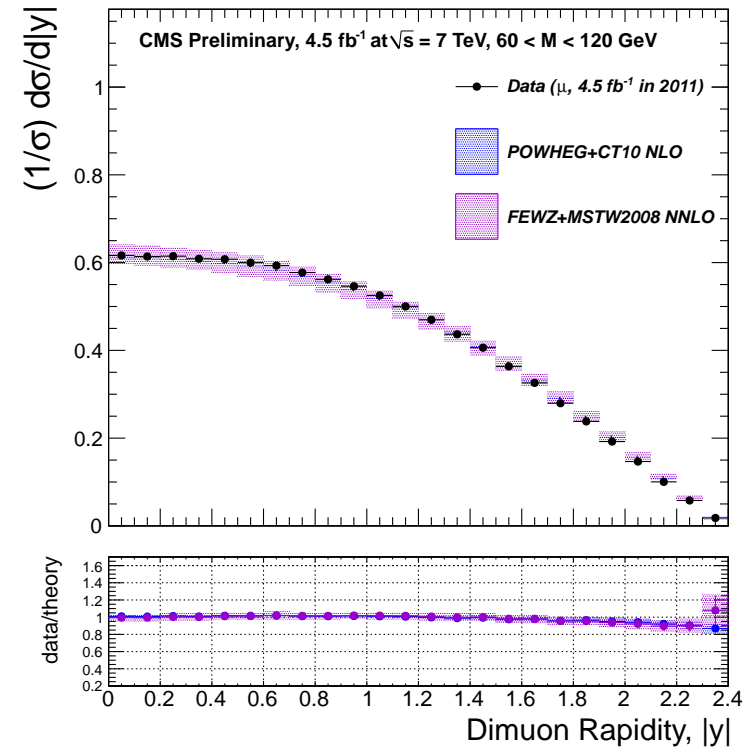
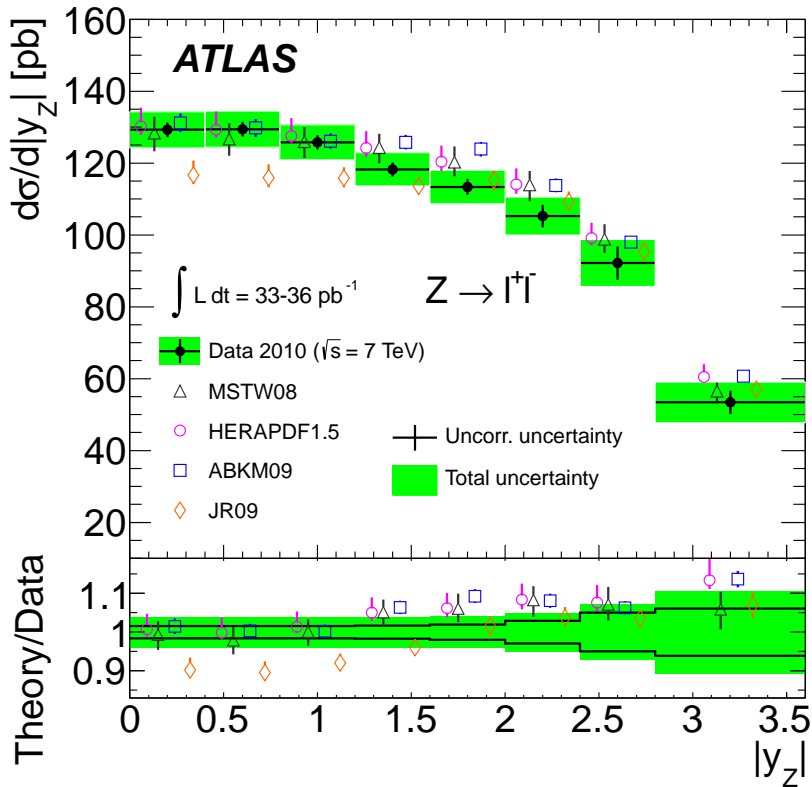


Measurement of W^+ and W^- production cross sections differentially in lepton rapidity η_ℓ give access to u_v and d_v PDFs. ATLAS measurements based on 2010 data can be translated to charge asymmetry A_l , given for $p_t^\ell > 20 \text{ GeV}$, $p_t^\nu > 25 \text{ GeV}$ while CMS result based on 2011 data is for $p_t^\ell > 35 \text{ GeV}$.



ATLAS, Phys. Rev. D85 (2012) 072004, CMS, arXiv:1206.2598

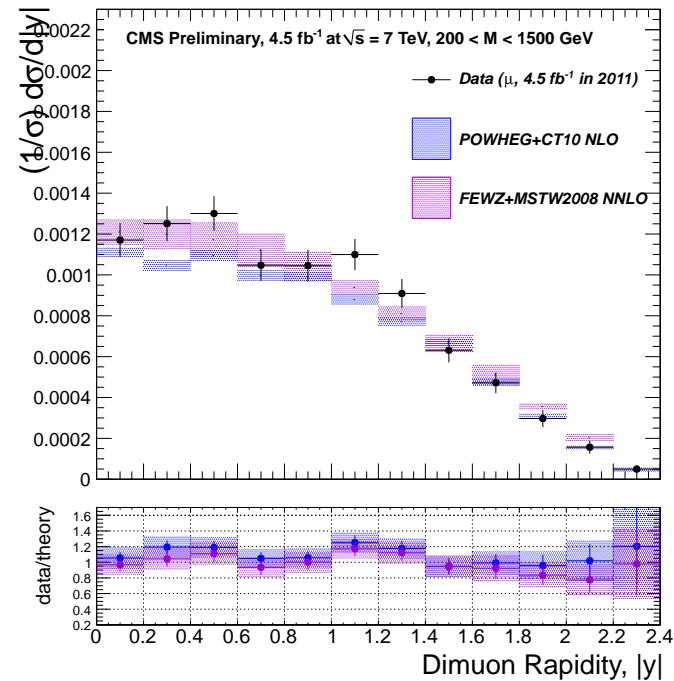
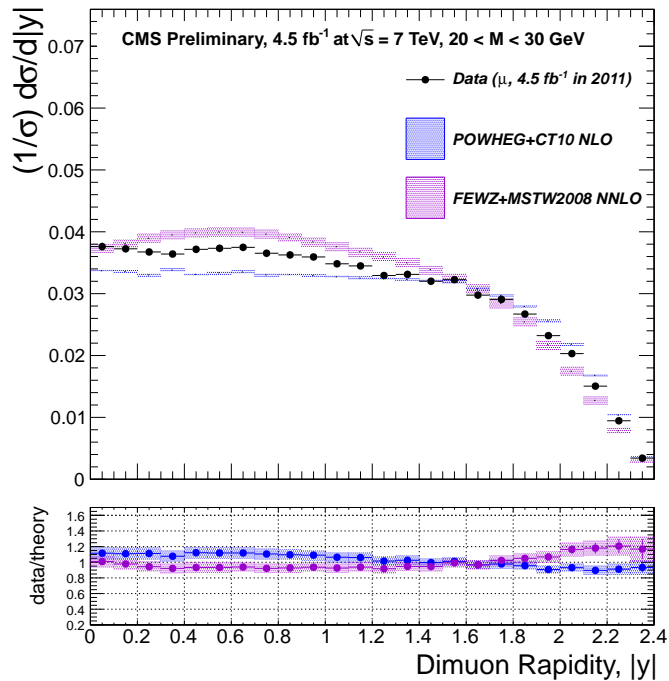
Differential Cross Sections: Z



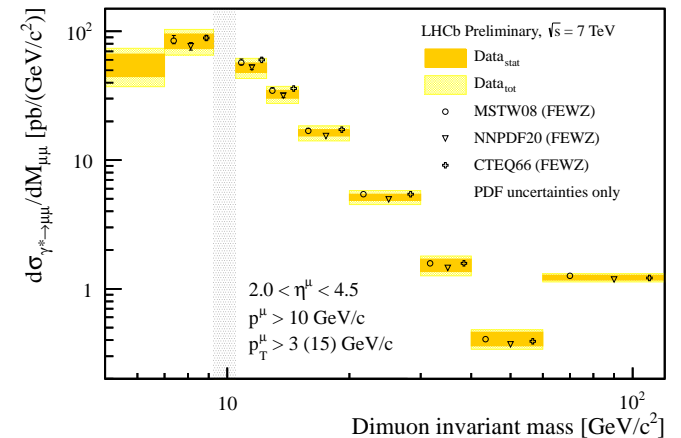
Compared to measurements of the F_2 structure function at HERA, which is dominated by γ exchange, Z production at the LHC is more sensitive to d -type quarks, provides information on \bar{d} , \bar{u} and s decomposition at $x \sim 0.01$. ATLAS reports absolute cross sections, based on 2010 data. CMS measures normalised cross sections, based on complete 2011 data sample.

ATLAS, Phys. Rev. D85 (2012) 072004, CMS PAS EWK-11-007

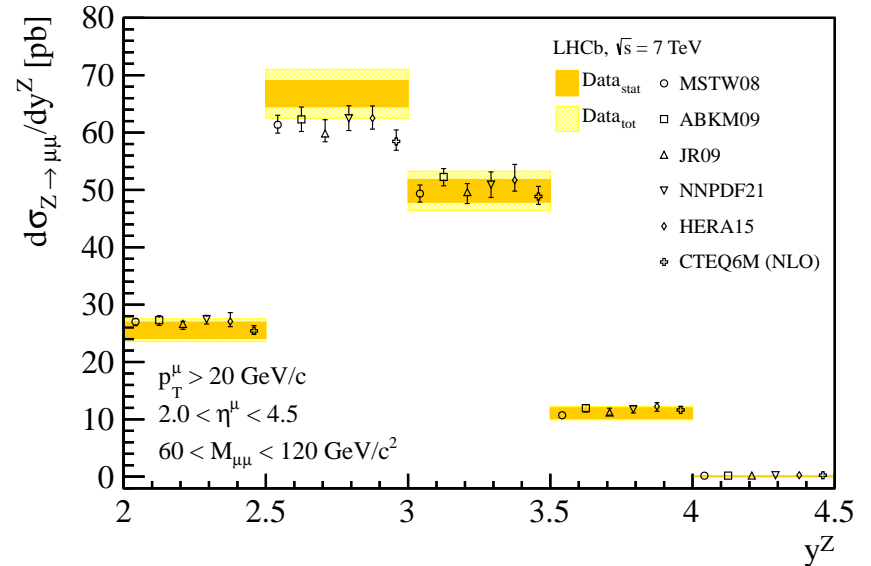
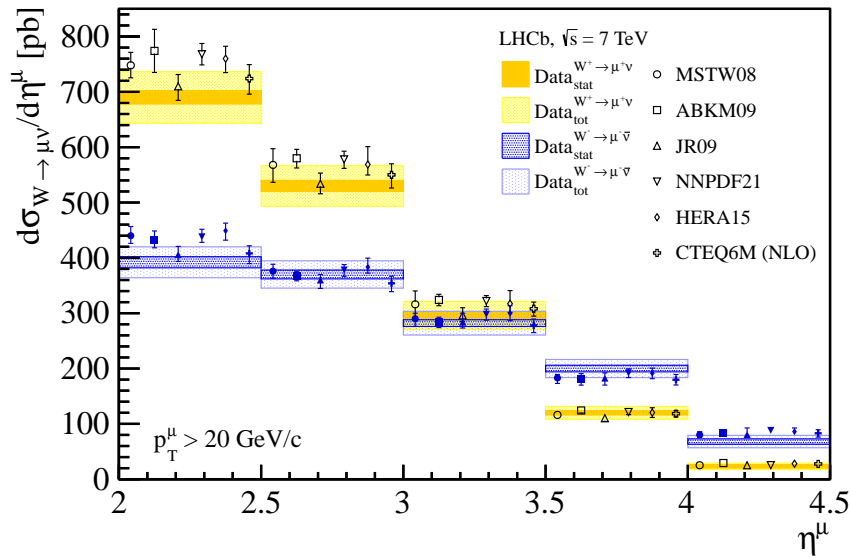
Differential Cross Sections: γ^*



Low mass DY process has similar PDF sensitivity to HERA data. CMS measures normalised $(1/\sigma)d\sigma/d|Y|$ for $20 < M_{\mu\mu} < 1500 \text{ GeV}$ range. The measurements are complemented by LHCb, which measures down to 5 GeV .



W, Z measurements from LHCb

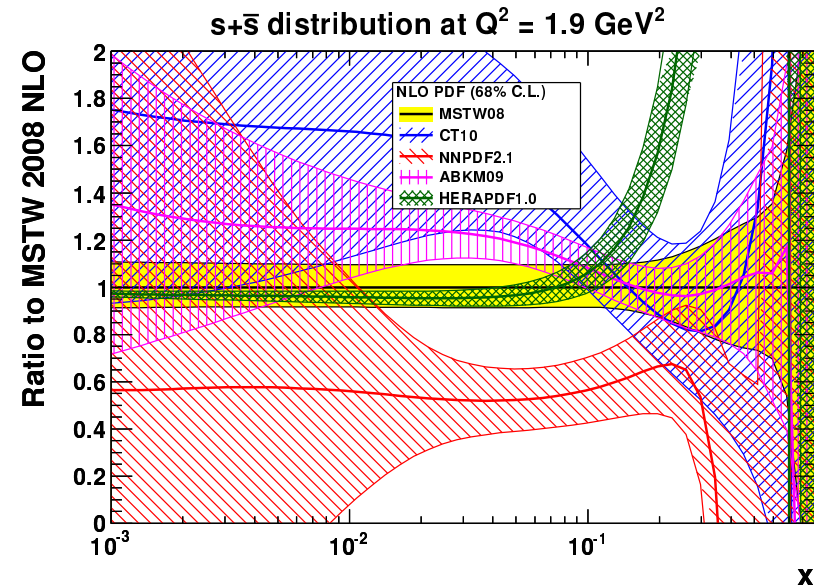
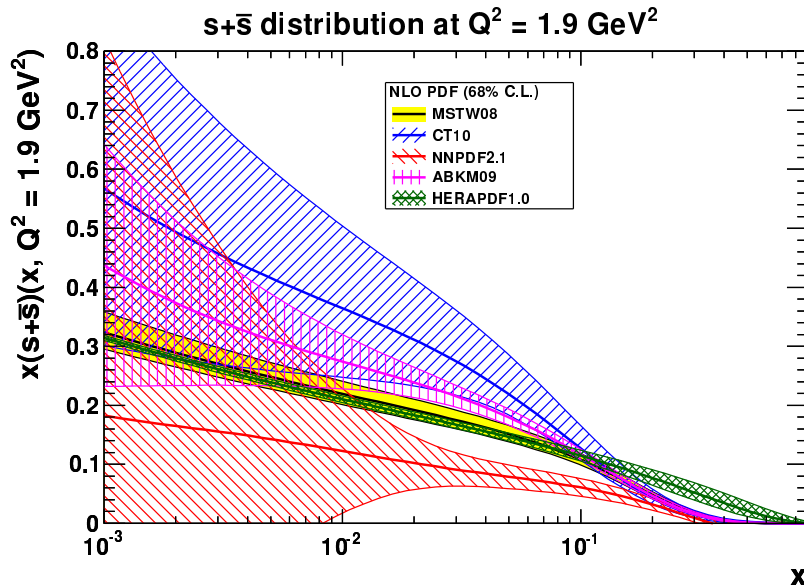


LHCb extends W differential cross-section measurement to $2 < \eta_\mu < 4.5$ range. For $\eta_\mu > 3.5$, W^- cross section exceeds W^+ due to V-A structure of W production.

ATLAS and CMS measure up to $y_Z = 3.6$ using central-forward topology of the scattered electrons; LHCb measures in the same range for symmetric configurations of the scattered muons: complimentary information for PDFs and electroweak fits.

LHCb, arXiv:1204.1620

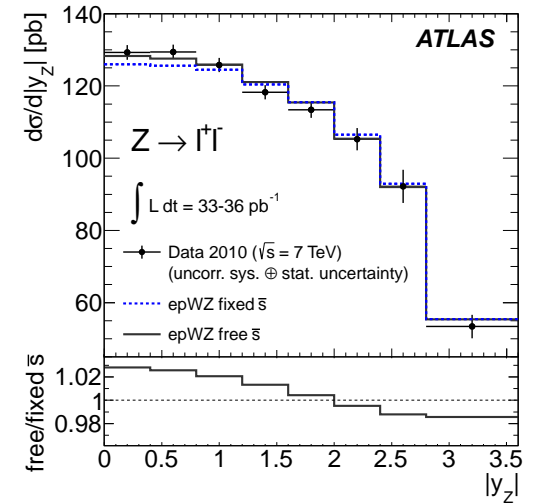
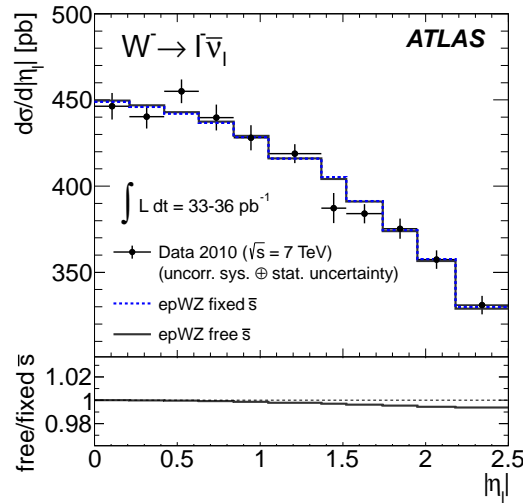
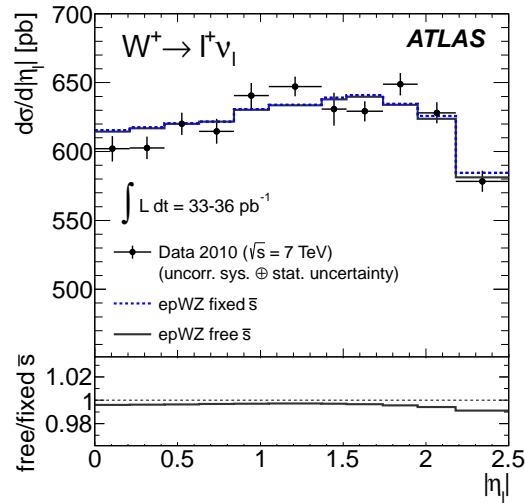
Strange density from different PDFs



Plots prepared by G. Watt

- Strange-sea density is determined from neutrino scattering, $\nu N \rightarrow X\mu^+\mu^-$ with dimuon final state, with the second muon produced from the charm decay.
- These data are included in PDF fits leading, however, to results which are hardly consistent with each other,

Determination of the strange-sea density



Perform two NNLO fits: with fixed strangeness fraction

$r_s = 0.5(s + \bar{s})/\bar{d}$, $r_s = 0.5$ and free strange density parametrized as

$$x\bar{s}(x) = A_s x^{B_{\bar{d}}}(1-x)^{C_s}$$

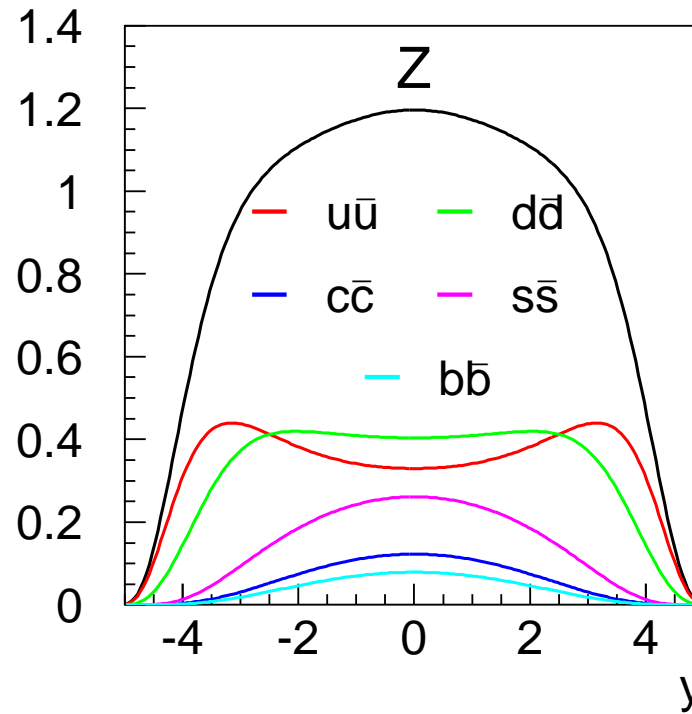
For $x = 0.023$ and $Q^2 = 1.9 \text{ GeV}^2$, corresponding to the maximum of ATLAS data sensitivity extrapolated to low Q^2

$$r_s = 1.00 \pm 0.20_{\text{exp}} \pm 0.07_{\text{mod}}^{+0.10}_{-0.15} \text{par}^{+0.06}_{-0.07} \alpha_s \pm 0.08_{\text{th.}}$$

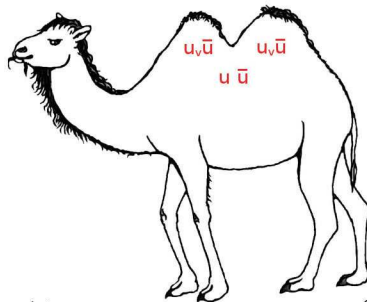
consistent with sea quark flavour democracy at low x .

ATLAS, arXiv:1203.4051

Flavor decomposition of the Z production at the LHC



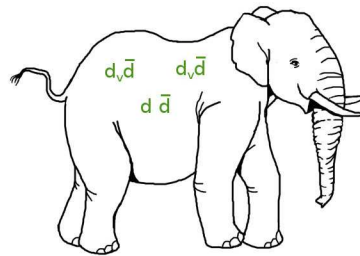
Color the Bactrian Camel



www.exploringnature.org

©Sheri Amsel

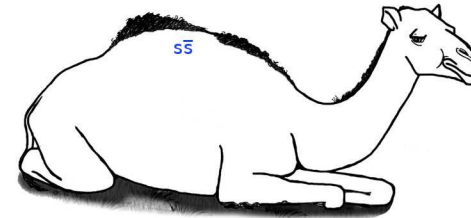
Color the Asian Elephant



©Sheri Amsel

www.exploringnature.org

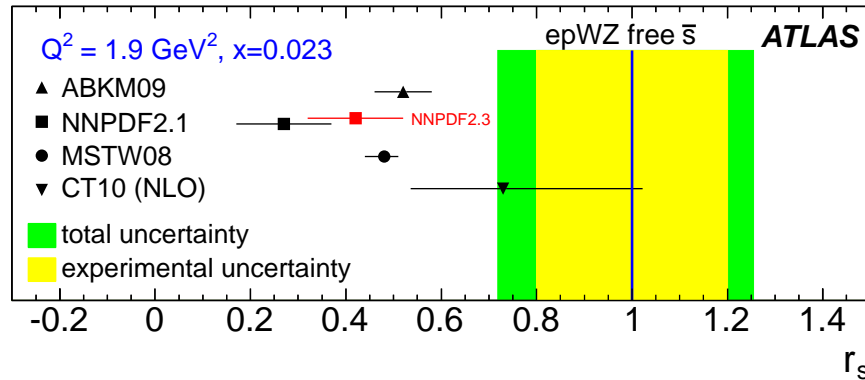
Color the Dromedary Camel



www.exploringnature.org

©Sheri Amsel

Strange-sea determination at the LHC



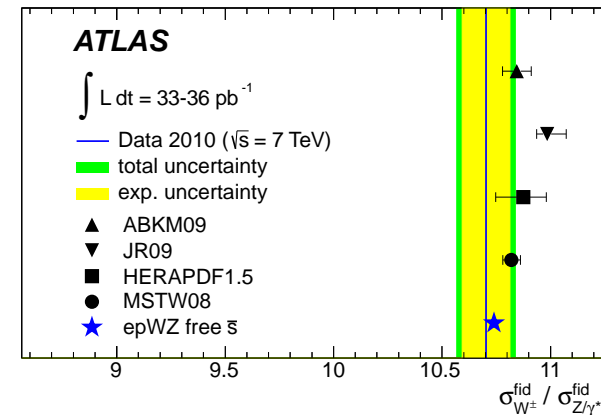
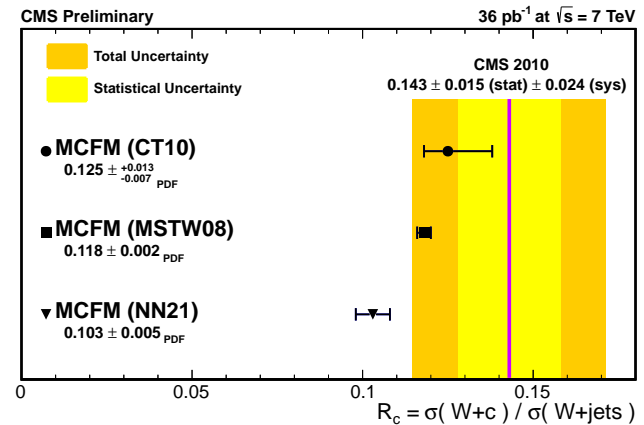
$$r_s = 0.5 \frac{s + \bar{s}}{\bar{d}}$$

ATLAS uses PDF fit to inclusive W, Z measurements. CMS result is based on $W + c$ production.

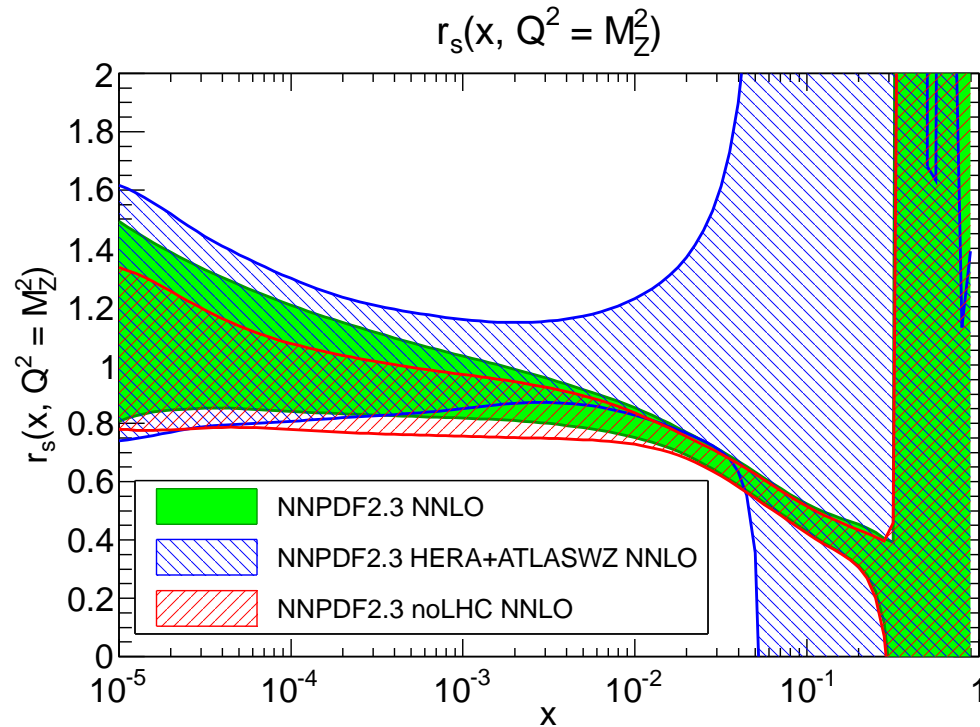
NNPDF2.3 result uses improved m_c threshold correction, affecting dimuon data (dominant effect) and includes ATLAS result (smaller effect).

ATLAS fit provides the best description of the measured W/Z cross sections ratio.

ATLAS, arXiv:1203.4051 CMS PAS EWK-11-013



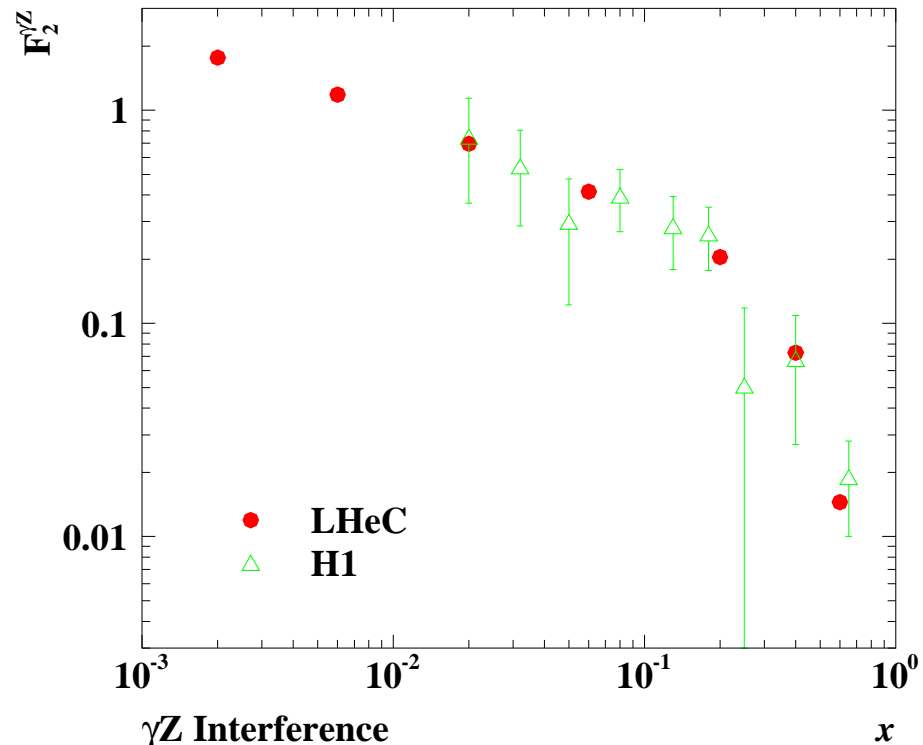
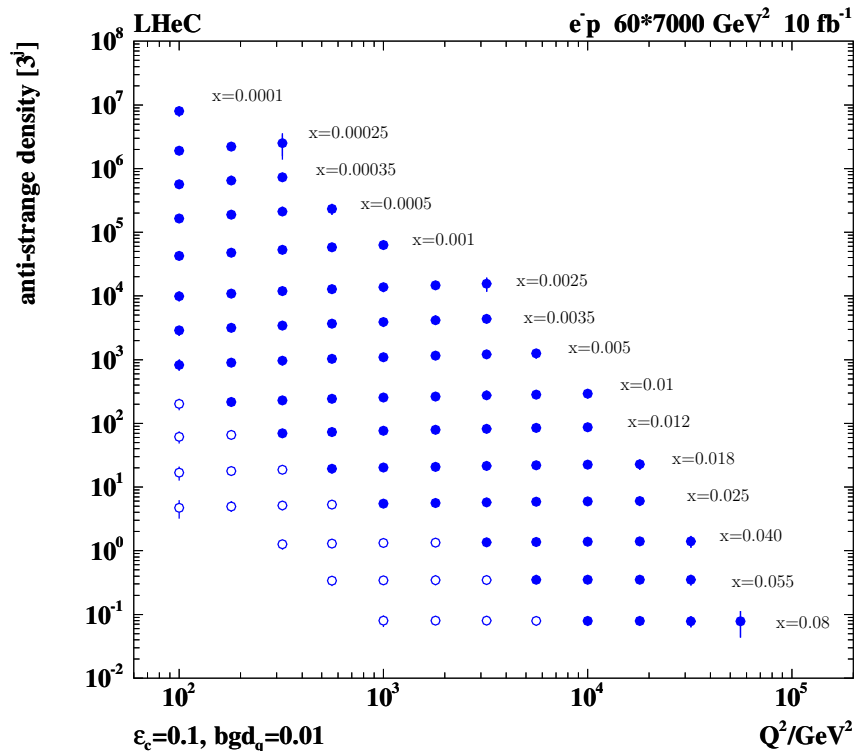
NNPDF2.3 Strangeness Study



NNPDF analysis also studies strangeness fraction, fitting HERA+ATLAS only and in a global fit. For $Q^2 = M_Z^2$ and $x = 0.013$ NNPDF finds for ATLAS+HERA fit $r_s = 1.04 \pm 0.23$ which has larger uncertainty compared to the ATLAS result $r_s = 1.00^{+0.08}_{-0.09}$. The maximum sensitivity on strangeness fraction for NNPDF analysis is at $x \sim 0.005$, the ATLAS data pulls strangeness of the combined fit at low x .

NNPDF Collaboration, arXiv:1207.1303

LHeC: high energy frontier for ep physics



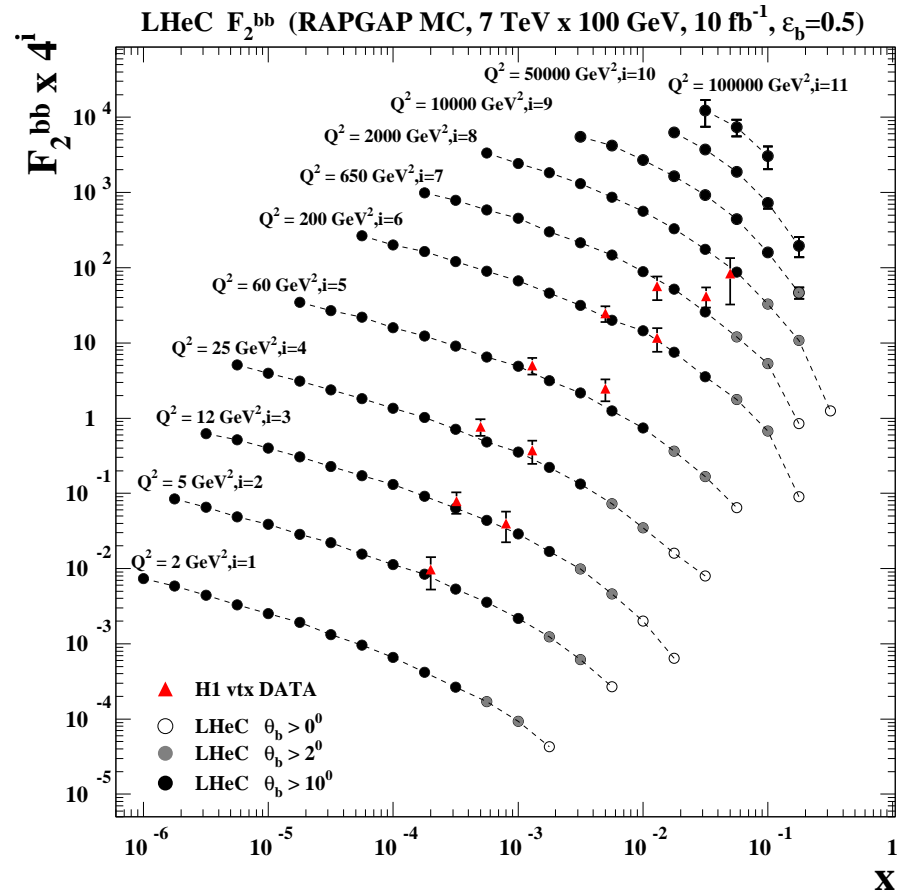
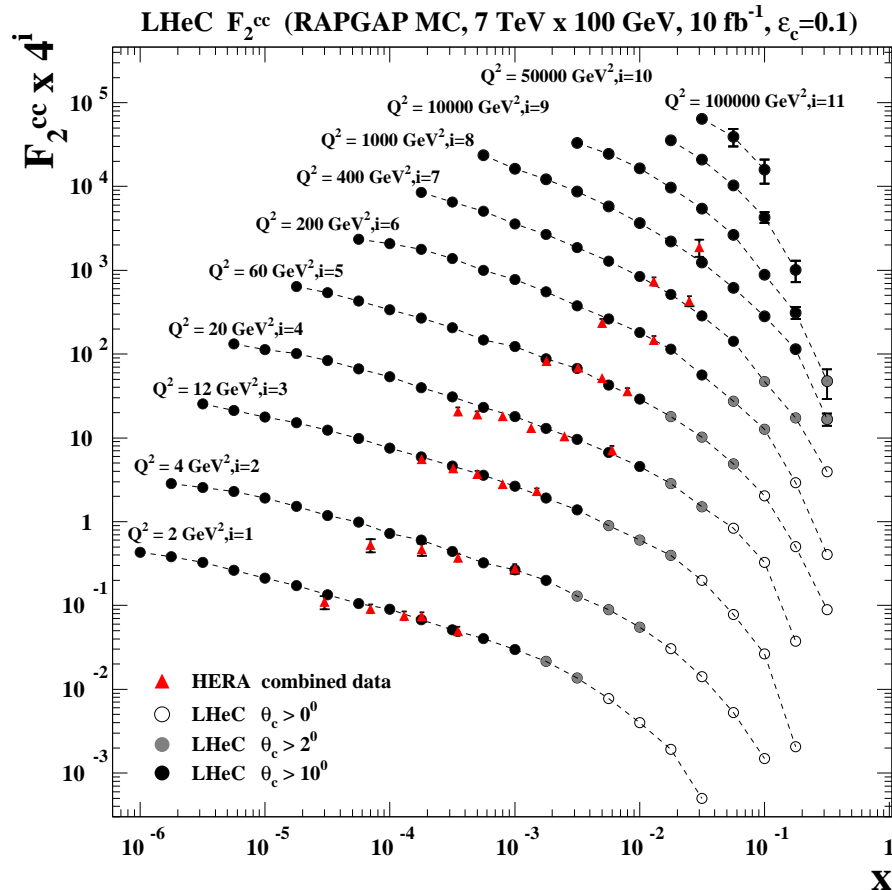
Future of DIS depends on proposed collider projects: EIC and LHeC.

LHeC is the high energy frontier which would use **7 TeV** protons from LHC and **60 GeV** polarised electrons from a dedicated racetrack linac.

The large center-of-mass energy of the LHeC together with high luminosity allows to measure strange density, using CC process with tagged charm.

Polarisation of the electron beam provides a way to measure $F_2^{\gamma Z}$ accurately.

LHeC — expected measurement of heavy flavours.



Large center-of-mass energy means that LHeC would access very low x at low Q^2 . Combined with heavy flavour tagging, this would provide unique opportunity to measure heavy flavours from the threshold region and Bjorken- x down to 10^{-6} up to EW scales.

LHeC study group arXiv:1206.2913

Summary

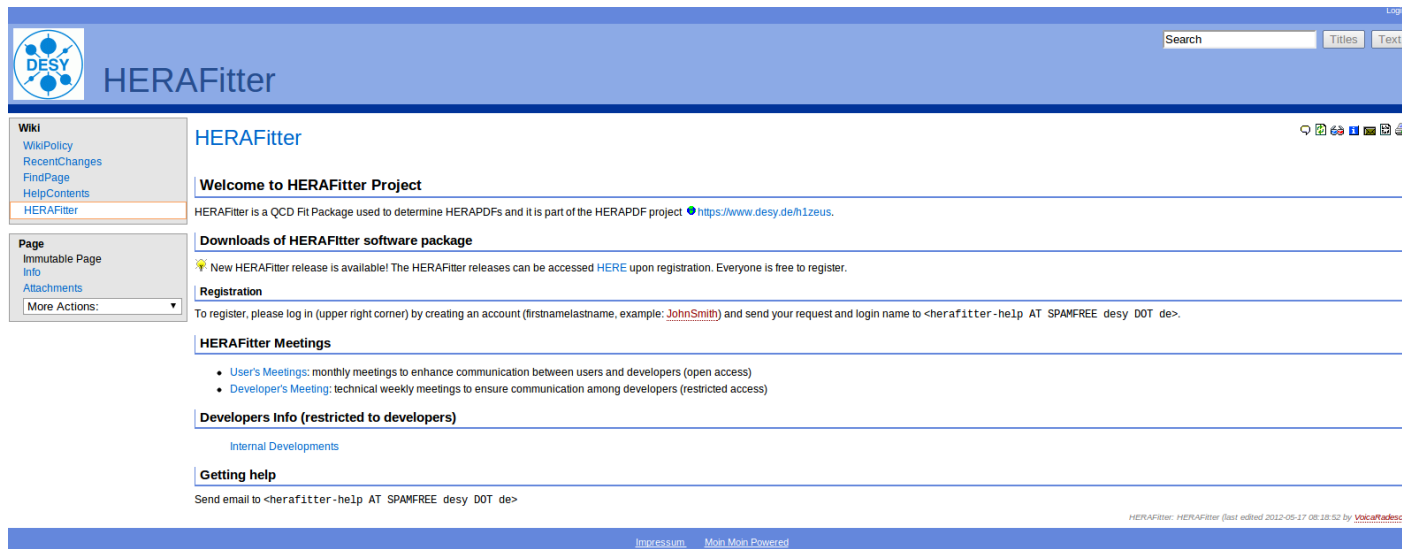
- HERA data provide essential information on the proton structure for the LHC. The analysis of the HERA inclusive data enters final stages.
- Predictions for the LHC are overall in good agreement with the data. LHC results start to have constraining power e.g on strange-sea density, valence PDFs.
- Future *ep* colliders promise large improvements in the understanding of the proton structure.

Extras

HERAFitter Open Source Code

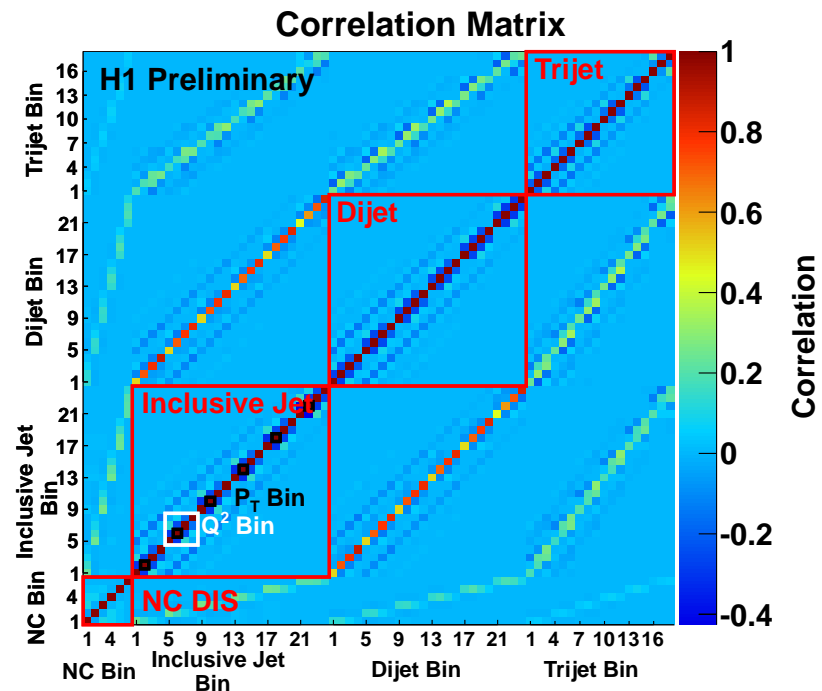
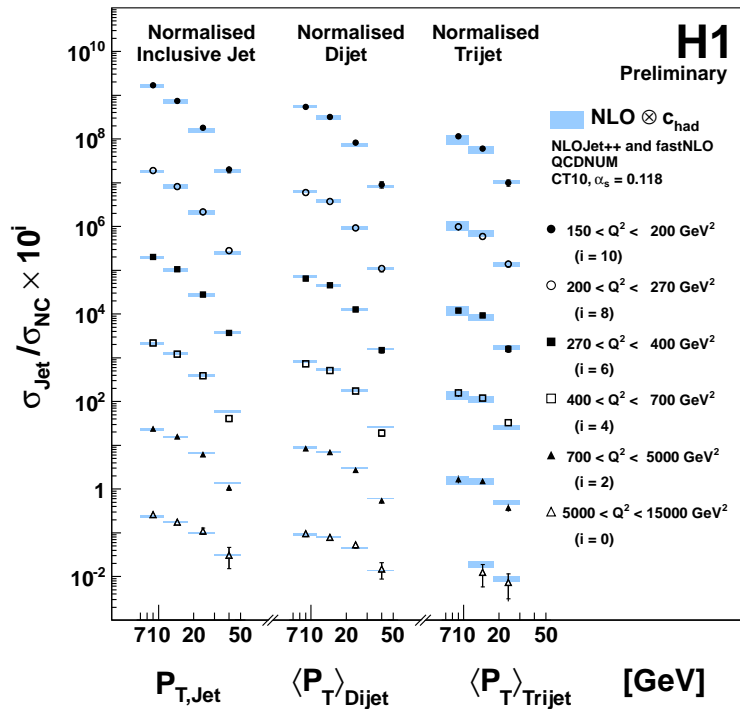
- HERAFitter code is available for download from [hepforge](#)
- Beta-2 version of the code is based on QCDNUM17 for parton evolution, contains codes from MSTW, CTEQ, ABKM for structure function calculation. LHC processes can be included using APPLGRID, FastNLO (for jets and DY) and Hathor (for $t\bar{t}$) interfaces.

→ a tool for benchmarking and QCD analysis of LHC data.



The screenshot shows the HERAFitter project page on the DESY wiki. The page features a blue header with the DESY logo and the text "HERAFitter". A search bar is located in the top right corner. On the left side, there is a navigation menu with links for "Wiki", "WikiPolicy", "RecentChanges", "FindPage", "HelpContents", and "HERAFitter". Below the menu, there are sections for "Page" (Immutable Page, Info, Attachments, More Actions) and "HERAFitter". The main content area includes a "Welcome to HERAFitter Project" section, a "Downloads of HERAFitter software package" section, a "Registration" section, a "HERAFitter Meetings" section, a "Developers Info (restricted to developers)" section, and a "Getting help" section. The footer contains the text "HERAFitter: HERAFitter (last edited 2012-05-17 08:18:52 by [VokarAdesky](#))" and "Impressum Main Menu Powered".

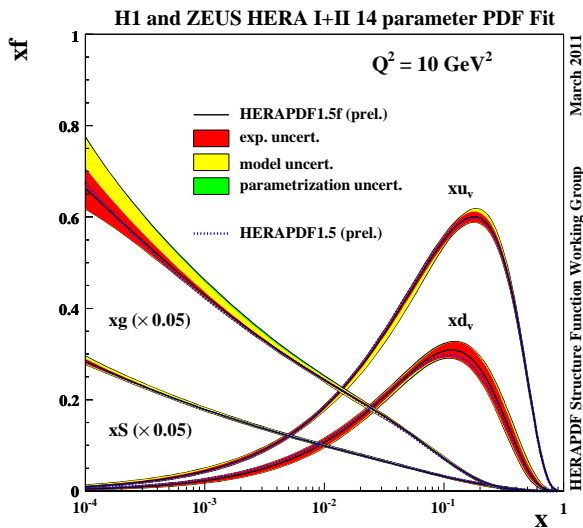
HERA jet measurements



H1Prelim-12-031

- Main information on the gluon density comes from scaling violation at HERA.
- Jet cross section can be also used to control gluon density, measure α_S .
- Correlated measurement of inclusive, di- and trijets by H1.

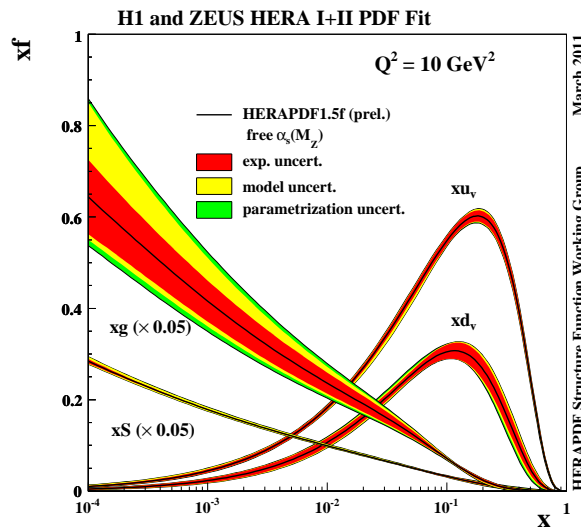
Combined Jet+DIS inclusive fit and $\alpha_S(m_Z)$



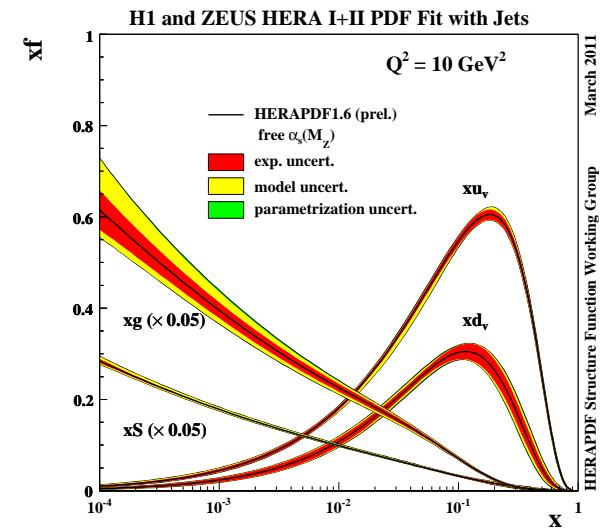
Fix α_S , no jets

H1prelim-11-034, ZEUS-prel-11-001

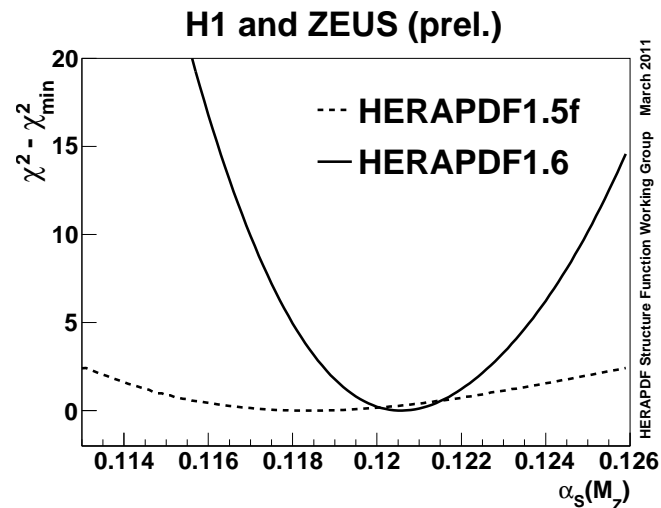
- Freeing α_S in fits increases $xg(x)$ uncertainty at low x due to large $xg(x)$ - α_S correlation.
- Inclusion jets allows to reduce this correlation and improve uncertainty.
- $\alpha_S(M_Z) = 0.1202 \pm 0.0013(\text{exp}) \pm 0.0007(\text{mod}) \pm 0.0012(\text{had})^{+0.0045}_{-0.0036}(\text{th})$.



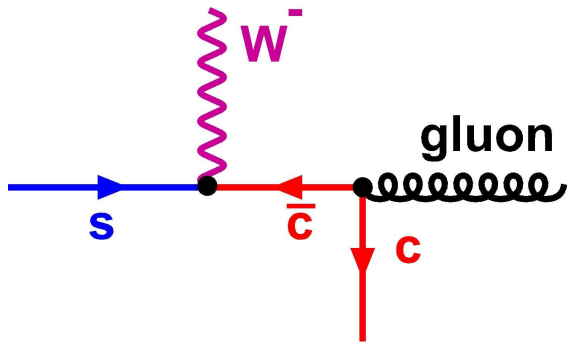
Free α_S , no jets



Free α_S , + jets



Probing proton strangeness at the LHC



Direct probe, using $W + c$ -jet production. CMS measures

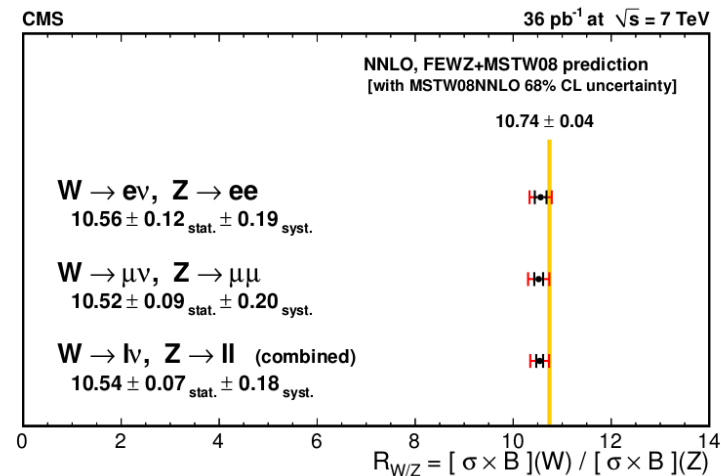
$$R_c = 0.143 \pm 0.015_{\text{stat}} \pm 0.024_{\text{syst}}$$

vs expectation, based on CT10,

$$R_c = 0.13 \pm 0.02.$$

CMS PAS EWK-11-013

Indirect probe, using different W and Z cross-section dependence, from their correlated measurement. For W/Z ratio, smaller values are expected for larger strangeness fraction since Z production is more affected than W .



CMS, JHEP 10 (2011) 007

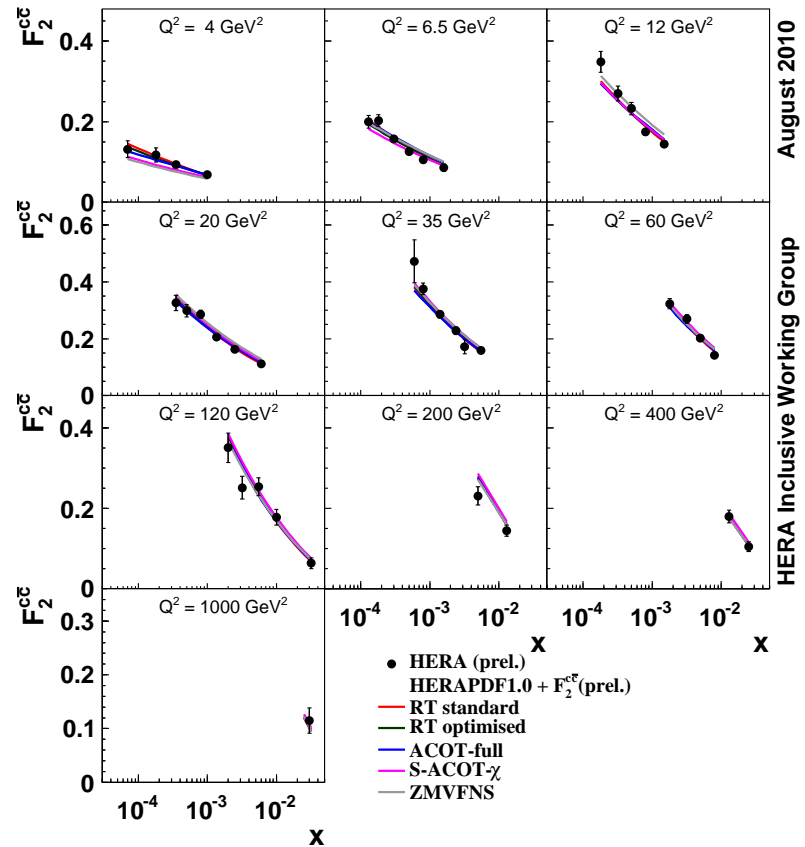
Decomposing u and c densities at low x

Inclusive structure function F_2 is sensitive to

$$F_2 \sim 4(U + \bar{U}) + (D + \bar{D}),$$

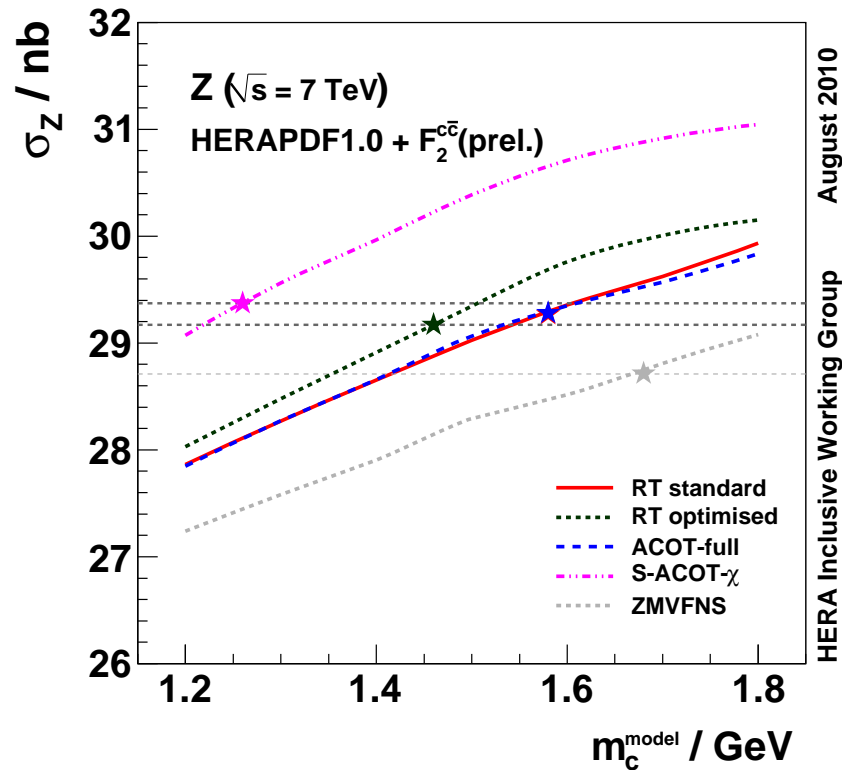
where $U = u + c$ and $D = d + s + b$. At low x , contribution of charm to F_2 reaches 30%.

The charm density can be calculated given the gluon density, however description of the charm threshold is complicated leading to a number of matching schemes (RT, ACOT, FNOLL...).



Combined HERA F_2^{cc} data reaches 5 – 10% precision per point, can be used to study different HF models.

W, Z cross sections and charm-sea density.



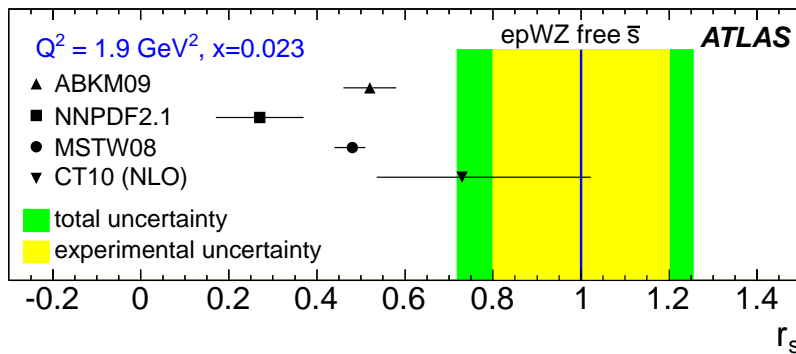
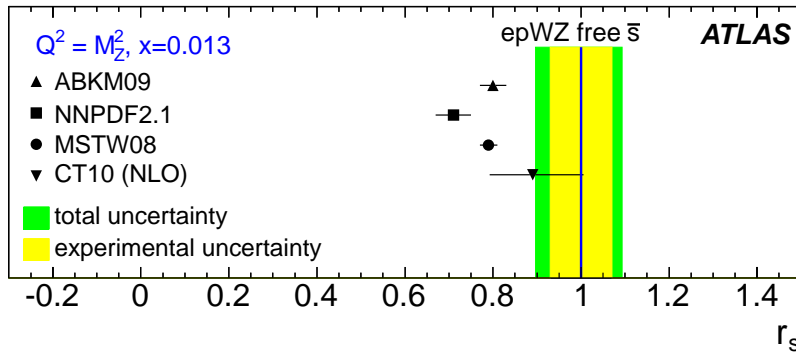
Fit the m_c^{model} parameter for various models such that they describe HERA data.

Large $\sim 7\%$ spread of the Z total cross section prediction at the LHC for m_c^{model} scan between $1.2 - 1.8 \text{ GeV}$ and also for a fixed m_c^{model} when considering different models.

However, the spread is reduced significantly when predictions are evaluated at the $m_c^{\text{model}}(\text{opt})$ values.

H1prelim-10-143, ZEUS-prel-10-019

ATLAS r_s result at $Q^2 = 1.9 \text{ GeV}^2$ and $Q^2 = M_Z^2$



ATLAS data have largest sensitivity to the strangeness fraction r_s for $Q^2 = M_Z^2$ and for $y_Z = 0$ corresponding to $x = 0.013$.

Due to the QCD evolution, this corresponds to $x = 0.023$ at $Q^2 = 1.9 \text{ GeV}^2$

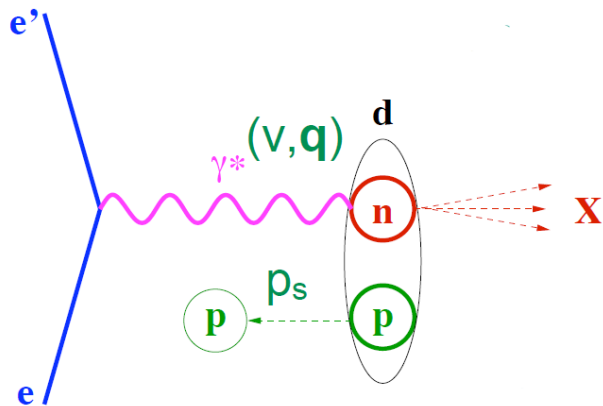
Flavour-blind gluon splitting process reduces and initial strangeness suppression as PDFs evolve to higher scales. Consequently, the uncertainties are also reduced, by about factor 2, for $Q^2 = M_Z^2$ compared to $Q^2 = 1.9 \text{ GeV}^2$, for all PDF sets.

Measurement of the neutron structure — tagged proton

- d/u limit for $x \rightarrow 1$ probes different theory predictions, important for high energy predictions (e.g. jet rates, W -mass).
- Measured using F_2^n/F_2^p assuming isospin symmetry:

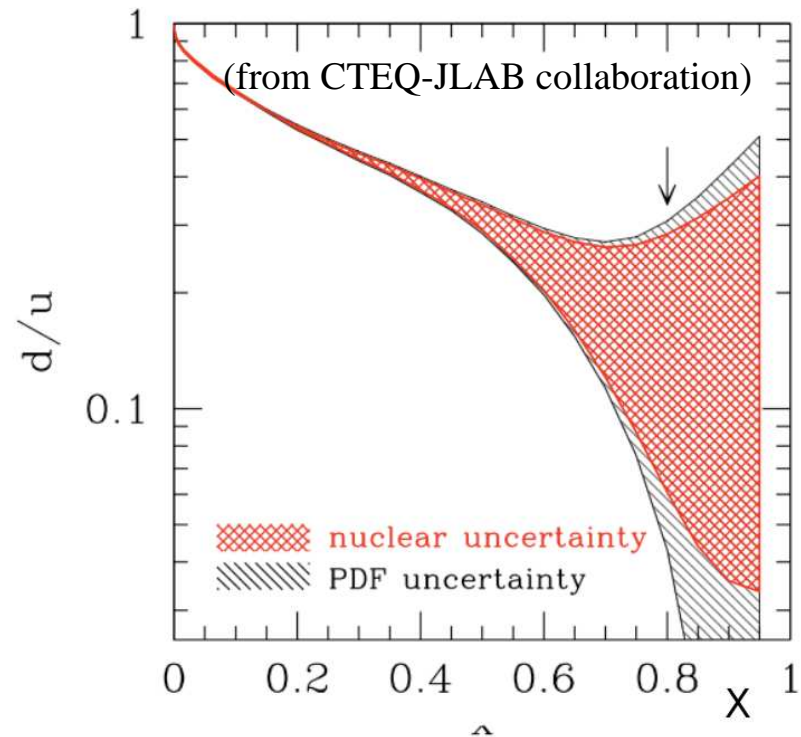
$$\frac{F_2^n}{F_2^p} = \frac{u + \bar{u} + 4(d + \bar{d}) + s + \bar{s}}{4(u + \bar{u}) + d + \bar{d} + s + \bar{s}}$$

However, large uncertainties due to nuclear corrections (EMC effect).

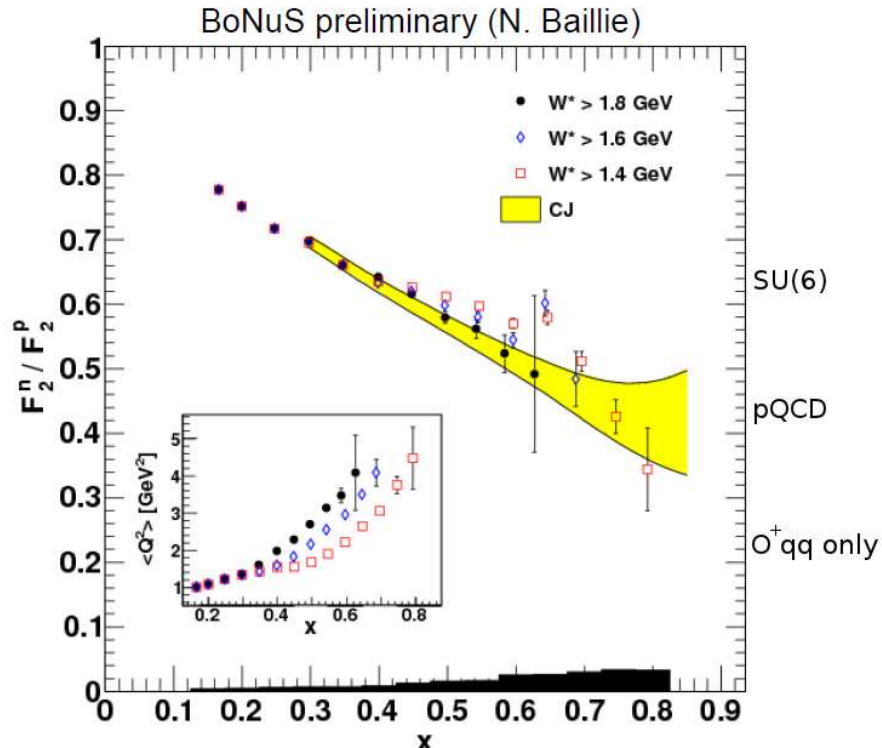


Detect the spectator proton from deuterium following en scattering. Use spectator proton momentum to correct kinematics. This can be done at colliders, EIC and LHeC, too.

BoNuS experiment using CLAS.



BoNuS and MARATHON



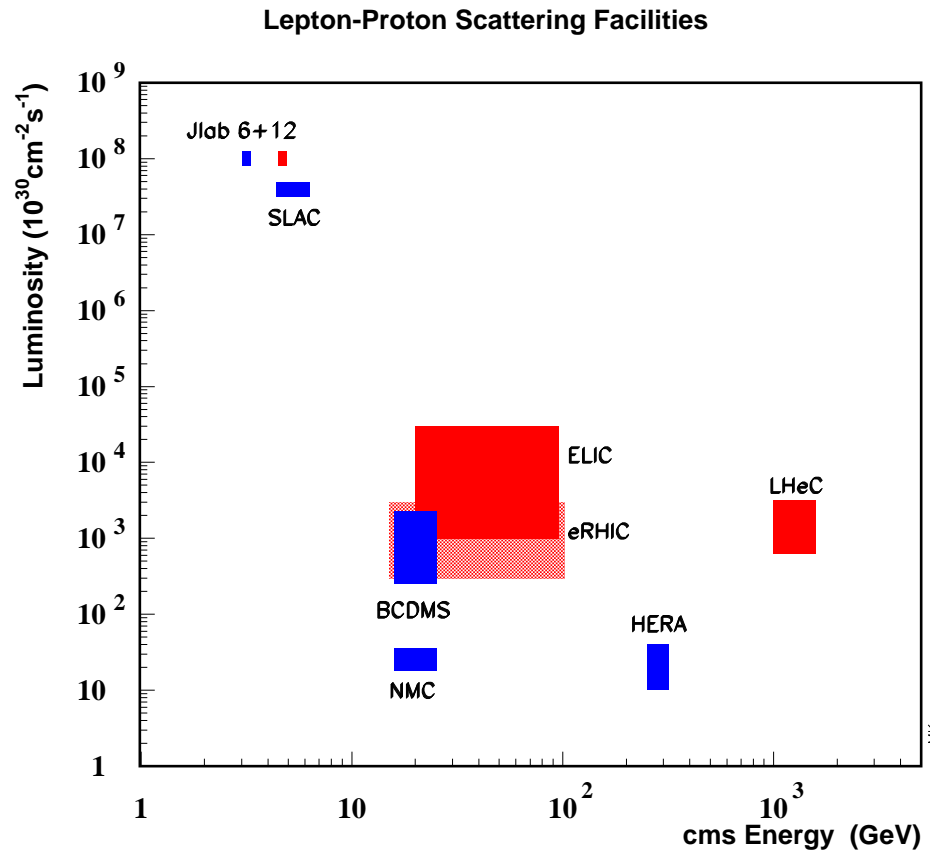
- First results from the BoNuS collaboration, using CLAS at hall B.
- Results approximately agree with CTEQ-JLAB analysis
- Higher beam energy is needed to measure at higher x and $W > 2 \text{ GeV}$.

Another approach: use SuperRation R^* :

$$\frac{\sigma^{He^3}}{\sigma^{H^3}} \approx \frac{F_2^{He^3}}{F_2^{H^3}} = R^* \frac{2F_2^p + F_2^n}{F_2^p + 2F_2^n}$$

which is expected to be close to 1 to $< 1.5\%$. Proposed to be measured by MARATHON with $E_e = 12 \text{ GeV}$.

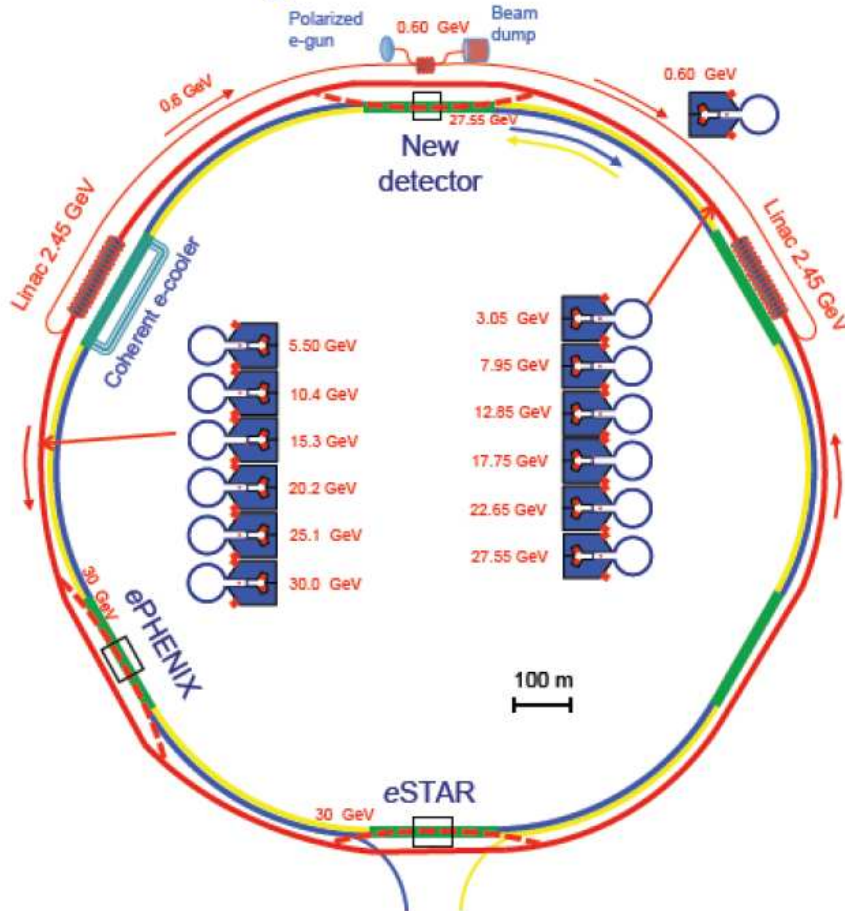
Future ep colliders



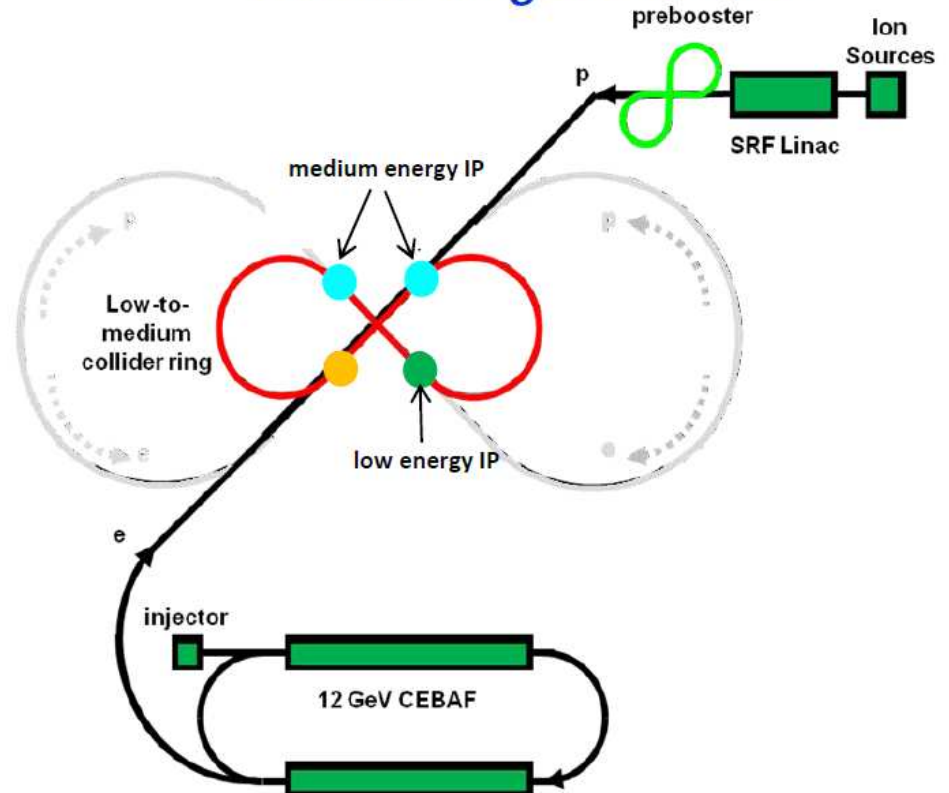
- Much increased luminosity for EIC and LHeC colliders compared to HERA.
- Increased center of mass energy for the LHeC allows for accurate measurements in electroweak regime.

EIC

eRHIC @ BNL: *add electron Energy Recovery Linac in RHIC tunnel*



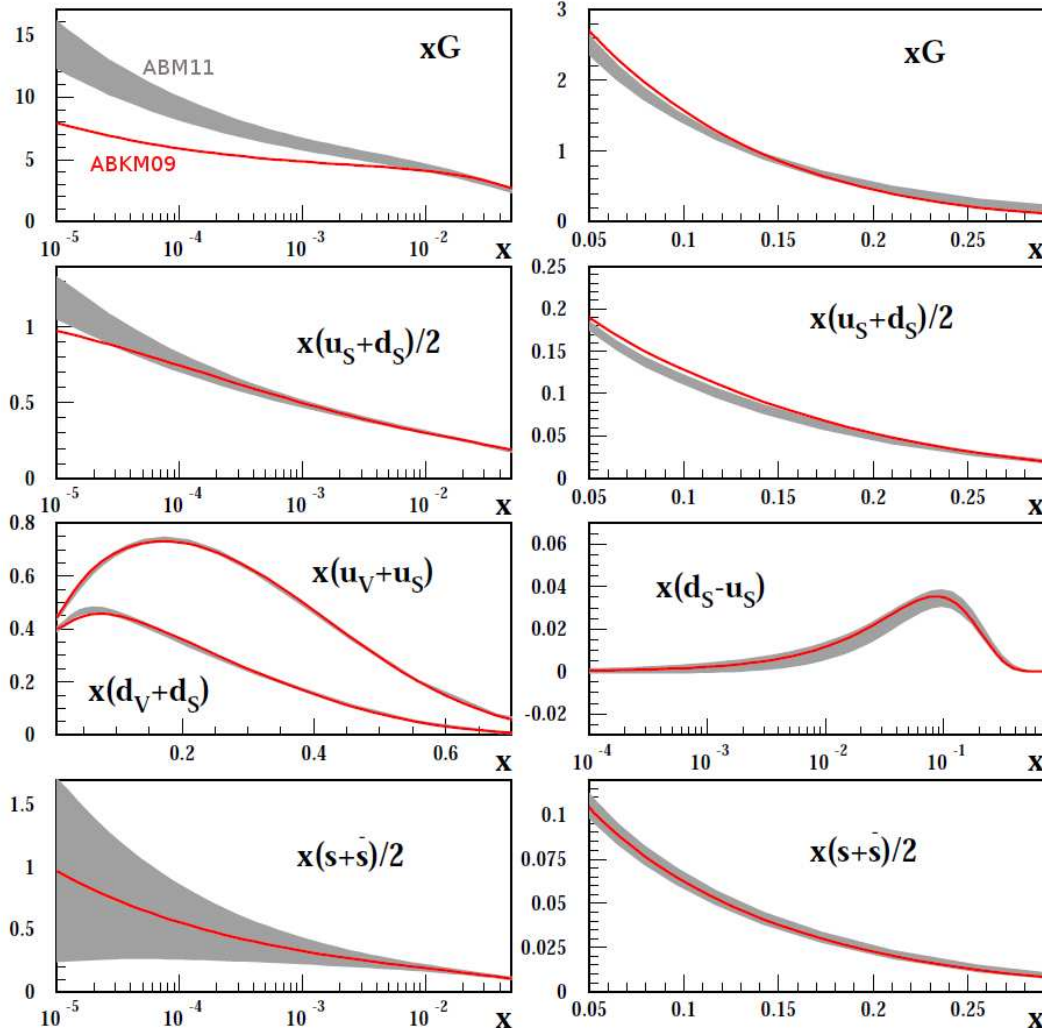
ELIC @ JLab: *add figure-8 hadron & electron rings to CEBAF*



Two designs for EIC collider. Both designs consider flexible setting for E_p , to measure F_L accurately.

ABM11 set

$\mu=2 \text{ GeV}, n_f=4$



S. Alekhin, J. Blümlein, S. Moch, arXiv:1202.2281

ABM11 is a recent update of the analysis based on non-LHC data. Comprehensive analysis with a detailed study of experimental uncertainties. Some changes vs previous ABKM09 set (shown as a red line) are due to usage of combined HERA data and improved treatment of heavy flavours.